M.R.P. 1078
S.C.11/246
15th November, 1957

METEOROLOGICAL OFFICE
28 JUN 1958
LERWICK OBSERVATORY
SHETLAND

Conservation of Vorticity at 100 mb

by

J. R. Probert-Jones

(Meteorological Office)

AIR MINISTRY

METEOROLOGICAL RESEARCH COMMITTEE

At the time of issue this report has not been published. Any author desiring to quote this paper should refer to it as "A paper of the Meteorological Research Committee (London), M.R.P. No. 1078 by Mr. J.R. PROBERT-JONES A copy is available in the Library of the Meteorological Office."

M.R.P.1078
S.C.II/246
15th November, 1957

AIR MINISTRY

METEOROLOGICAL RESEARCH COMMITTEE

Conservation of Vorticity at 100 mb

by

J. R. Probert-Jones (Meteorological Office)

1. Introduction

The purpose of the experiment described in this report has been to ascertain whether the flow at 100 mb can be treated as essentially non-divergent. The method of attack has been to determine whether sequences of 100 mb charts can be so drawn that (geostrophic) absolute vorticity is conserved in the motion. The graphical technique developed by Fjortoft (1) has been used.

2. Theory

The vorticity equation in non-divergent flow, neglecting vertical motion, is

$$\frac{\partial \eta}{\partial t} + \underline{V} \cdot \underline{\nabla} \eta = 0, \qquad (1)$$

where η is the absolute vorticity.

If we consider geostrophic motion in an isobaric surface,

$$\eta = \frac{g}{l} \nabla^2 z + l$$

and $\underline{V} = \frac{g}{l} \underline{k} \wedge \underline{\nabla} z$, where 'z' is the height of the isobaric surface, 'l' is the Coriolis parameter, and 'k' the unit vertical vector, equation (1) becomes:

$$\frac{\partial}{\partial t} \nabla^2 z = - J(z, \eta) \qquad (2)$$

If Z_i are the values of z at the four points of a square mesh of side 2h surrounding a point 0, a simple finite difference approximation to $\nabla^2 z$ is

$$\nabla^2 z = \frac{1}{h^2} \left(\sum_{i=1}^{4} Z_i - 4 Z_0 \right) = \frac{4}{h^2} \left(\bar{Z} - Z_0 \right),$$

where $$\bar{Z} = \frac{1}{4} \sum_{i=1}^{4} Z_i \ .$$

/Equation

Equation (2) gives:

$$\frac{\partial}{\partial t}\left(Z-\bar{Z}\right) = -\frac{l}{m^2}\,\underline{V}\cdot\underline{\nabla}\left\{\frac{m^2}{l}\left(Z-\bar{Z}\right)\right\} + \underline{V}\cdot\frac{lh^2}{4gm^2}\underline{\nabla}l, \quad (3)$$

where m is the scale factor of the map projection used. Putting:

$$G = \int_0^{\Theta} \frac{l^2h^2}{4gm^2}\cot\Theta\, d\Theta,$$

Θ being the latitude, and neglecting $(Z - \bar{Z})\underline{\nabla}\frac{m^2}{l}$ in comparison with $\frac{m^2}{l}\underline{\nabla}(Z - \bar{Z})$, equation (3) becomes:

$$\frac{\partial}{\partial t}\left(Z-\bar{Z}-G\right) = -\frac{g}{l}J\left(Z, Z-\bar{Z}-G\right)$$

$$= -\frac{g}{l}J\left(\bar{Z}+G, Z-\bar{Z}-G\right). \quad (4)$$

Equation (4) shows that in non-divergent geostrophic flow the vorticity approximation $Z - \bar{Z} - G$ is conserved in the space-mean field $\bar{Z} + G$. This latter field is known from experiment to be more conservative than the Z field, and is assumed sufficiently constant to warrant displacement of the vorticity field in a single time-step of 12 hrs.

Contours of G are shown in Fig. 1.

It can be shown that the maximum value of $(Z - \bar{Z})\underline{\nabla}\frac{m^2}{l}$, the term neglected above, is about one-fifth of $\frac{m^2}{l}\underline{\nabla}(Z - \bar{Z})$.

3. Design of the experiment

It has been shown above that if the flow at 100 mb is non-divergent a certain function $Z - \bar{Z} - G$, representing the vorticity, will be conserved in the $\bar{Z} + G$, or smoothed flow, field. For convenience throughout this report the $Z - \bar{Z} - G$ field will be referred to as the vorticity field, although it is only a graphical approximation to this field.

Johnson (2, 3) finds that the root-mean-square random error of observation of height of the 100 mb surface over the British Isles is 150 ft, and that the vector root-mean-square error for wind observations is less than 6 kt. These errors and the scarcity of observations, particularly of wind, at this level, allow considerable latitude in the drawing of 100 mb contours. Therefore it was decided to examine a few sequences of routine 100 mb charts and to attempt to redraw them to be consistent with the hypothesis that absolute vorticity was conserved following the motion and yet retain consistency with the observations. Thus the vorticity given by any one chart should not differ, by more than a stipulated amount at any point, from the vorticity obtained by advection, forwards or backwards in time, from its immediate neighbour. It was anticipated that more than one modification to any one chart might be necessary.

If the charts could be so redrawn, a comparison could subsequently be made between the fitting of the wind and height reports in the original and modified drawings.

4. Method

100 mb charts for the six months November to April for the winters 1953-54,

/1954

1954-55 and 1955-56 were examined for sequences in which a fairly strong flow existed in the neighbourhood of the British Isles together with a well-marked feature in the flow pattern which would provide significant vorticity variations. A reasonable cover of observations was also sought. Five sequences were extracted and are detailed below.

1. 1500Z 16/12/55 to 1500Z 19/12/55. A trough to the west of the British Isles in the strong flow moved east and was replaced by a quasi-stationary ridge over the Atlantic.

2. 1500Z 5/2/54 to 1500Z 8/2/54. A trough developed to the west of Ireland and moved east slowly to lie over Central Europe.

3. 0300Z 4/11/55 to 1500Z 6/11/55. A deep trough with its axis from Iceland to the Azores remained quasi-stationary and developed a closed vortex.

4. 0300Z 14/2/54 to 0300Z 17/2/54. In the strong flow a ridge from the Azores to Iceland and a trough over the east of America moved east to cover the British Isles and the central Atlantic respectively.

5. 0300Z 8/11/55 to 1500Z 12/11/55. A trough to the west of Ireland decreased in amplitude while a ridge off Labrador moved east slowly.

A preliminary inspection of routine working charts suggested that too much emphasis had been placed on height values and too little on winds and that some alteration was allowable. This was therefore carried out for all sequences, care being taken to ensure continuity in time throughout each sequence. In the remainder of this report these redrawn charts will be referred to as 'original' charts. These charts for sequences (2) and (3) are shown in the Figures.

Estoqué (4) has detailed the method of obtaining graphically the required vorticity and advection fields. A grid-length of 600 mi. was used, and isopleths drawn at 100 ft intervals. One alteration was made to his procedure in the present case. Instead of forming the $\overline{Z}$ + G field by adding the G field to the $\overline{Z}$ field, a vary inaccurate process at the 100 mb level, the Z - G field was formed as an intermediate step. From this the Z-$\overline{Z}$-G field and thence the $\overline{Z}$ + G field is easily obtained.

The field of - (Z-$\overline{Z}$-G), corresponding to the vorticity, for the first chart of each sequence, was advected for a period of 12 hrs. On comparing this with the pattern of -(Z-$\overline{Z}$-G) for the second chart it was apparent that significant differences existed, of the order of 300 ft in places, and the patterns definitely did not resemble each other. Since the Z-$\overline{Z}$-G ispoleths were drawn at 100 ft intervals, it was decided to attempt to achieve correspondence within a tolerance of 100 ft which is equivalent to a divergence of about 2×10^{-6} sec^{-1}.

An attempt was then made to modify the second chart within the limits of the accuracy of the observations by altering the shear and curvature, to give a vorticity pattern similar to the advected one and within the 100 ft tolerance. In the first two sequences this was not possible in one step, and changes in the first chart in each sequence had to be made, using advection of vorticity backwards in time from a modified second chart, in order to keep within the 100 ft tolerance.

The vorticity of the modified second chart was then advected in the space-mean flow field and the third chart modified to give a vorticity pattern similar to the advected one. This procedure was continued for the rest of the sequence. The original and modified height charts, and the original, modified and advected vorticity charts, for sequences (2) and (3) are shown in Fig.3 to 30 and 31 to 52 respectively.

The method requires that the advective field can be treated as constant

/over

over the period of advection. Examination of these fields at 12 hr intervals showed that this was satisfied to a high order of accuracy.

5. Results

It was found possible to redraw the five sequences of 100 mb charts so that the change in each 12 hr period implied a divergence of less than 2×10^{-6} sec^{-1}, which is negligible on the synoptic scale. A visual comparison of the original, advected, and modified vorticity fields, shown for sequences (2) and (3) in the Figures, clearly reveals the great improvement given by the modified fields in comparison with the original fields in corresponding with the advected fields.

An indication of the relative accuracy of the two sets of 100 mb charts is given by a comparison of their smoothness in time. Values of height and geostrophic wind were read off at points of a grid shown in Fig.2 covering that part of the chart where the drawing was considered most reliable. Values of the statistics $(Z_{12} - Z_o)$, the modulus of the twelve-hour height change, and $(V_{12} - V_o)$, the modulus of the twelve-hour vector wind change, are given in Table I, where $\overline{|V|}$ is the mean of the wind-speeds.

Table I

Time variation in height and geostrophic wind from grid

Sequence	$(Z_{12} - Z_o)$		$(V_{12} - V_o)$			
	Average value ft.	r.m.s. value ft.	Average value kt.	r.m.s. value kt.	$\overline{\lvert V \rvert}$ kt.	No. of cases
I Original	184	241	16	20	44	72
I Modified	160	206	12	14	48	
II Original	167	211	14	18	39	72
II Modified	176	217	9	10	37	
III Original	158	183	12	15	29	60
III Modified	154	171	8	9	30	
IV Original	203	261	17	19	42	72
IV Modified	165	222	11	13	40	
V Original	178	207	10	12	29	108
V Modified	157	183	6	7	29	

A comparison between reported winds and heights, and those read off the two sets of charts at the seventeen stations O.W.S. 'A', 'B', 'C', 'D', 'E', 'I', 'J', 'K', Stornoway, Aldergrove, Hemsby, Camborne, Flensburg, Wiesbaden, Munich, Gibraltar and Malta, is given in Table II, where Zr, Vr refer to the heights and geostrophic winds read off the charts, and Zo, Vo the observed or reported values from the radiosonde ascents.

/Table

Table II

Comparison between observed and measured winds and heights

Sequence	(Zr - Zo) Average value ft.	(Zr - Zo) r.m.s. value ft.	(Zr - Zo) No. of cases	(Vr - Vo) Average value kt.	(Vr - Vo) r.m.s. value kt.	$(\overline{Vo})$ kt.	$\lvert\overline{Vr}\rvert$ kt.	(Vr - Vo) No. of cases
I Original	114	157	98	11	14	45	43	73
I Modified	158	196		10	12		42	
II Original	131	174	92	10	12	39	38	38
II Modified	167	210		11	12		34	
III Original	83	120	85	9	11	27	28	62
III Modified	98	134		9	11		26	
IV Original	101	148	78	13	15	40	40	48
IV Modified	136	187		11	12		38	
V Original	95	129	137	9	12	25	26	99
V Modified	109	145		8	10		24	

No deterioration in the fitting of the observations during the course of any sequence was found.

Johnson (2) shows that the root-mean-square random error of observation of height at 100 mb from British radiosondes is 150 ft, and this figure probably applies to the radiosondes of the other stations used in Table II. The results of the Payerne trials, however, show a significant systematic error between the radiosondes of different countries. Errors due to chart drawing and reading off the charts are small in comparison, and the expected value of (Zr - Zo) can be taken as greater than 150 ft by perhaps 20 to 30 ft.

Upper limits to the root-mean-square error of wind observations from British and British Ocean Weather Ship stations of 6 kt and 9 kt are given by Johnson (3). Errors due to chart drawing, a geostrophic motion and estimation of the geostrophic wind are not negligible, but it is probable that the expected value of (Vr - Vo) does not exceed 10 kt.

6. Conclusions

The twelve-hour root-mean-square variation of height and geostrophic wind of the original set of 100 mb charts is 222 ft and 17 kt respectively; for the set modified to be consistent with vorticity advection the figures are 200 ft and 11 kt. The observations of height and wind have been fitted with root-mean-square errors for the original set of 146 ft and 13 kt. and for the modified set of 175 ft and 11 kt respectively. The modified set is therefore smoother in time with respect to height and significantly smoother with respect to wind than the original set. The observed winds are fitted better by the modified drawings, and although the heights are fitted better by the original set, the discussion of the errors in the height values given above would seem to indicate that the fit of the original set is too good. On the basis of these figures it is suggested that the modified set provides a more realistic approximation to the true flow than the original set.

Any generalisation to conditions at the 100 mb level at other times is not strictly justified. Since, however, the sequences selected show very varying conditions and probably contain representative types of flow found at this level, it can be concluded that the evidence supports the hypothesis of approximate non-divergent flow at the 100 mb level.

/REFERENCES:

REFERENCES:

1. Fjortoft, R. 1952. "Numerical Method of Integrating the Barotropic Vorticity Equation." Tellus 4, No. 3.

2. Johnson, D.H. 1954. "Accuracy of 100 mb Contour Heights." Met. Mag., Vol. 83, p.37.

3. Johnson, D.H. 1953. "Accuracy of 100 mb Winds." Met. Mag. Vol. 82, p.44.

4. Estoqué, M.A. 1956. "A Prediction Model for Cyclone Development Integrated by Fjortoft's Graphical Method." J. Met., Vol. 13, No.2.

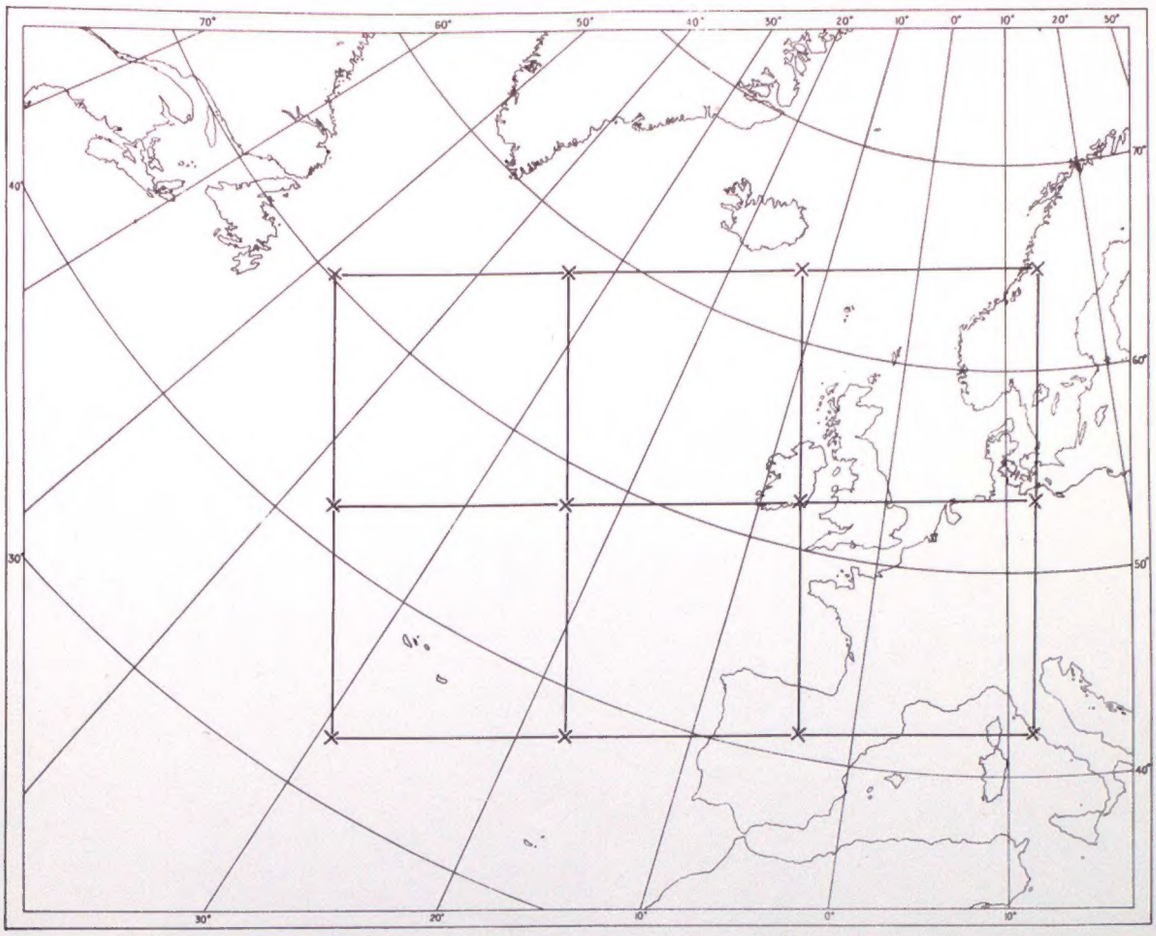

Fig.2. Grid used in testing the time variations of contour height and geostrophic wind

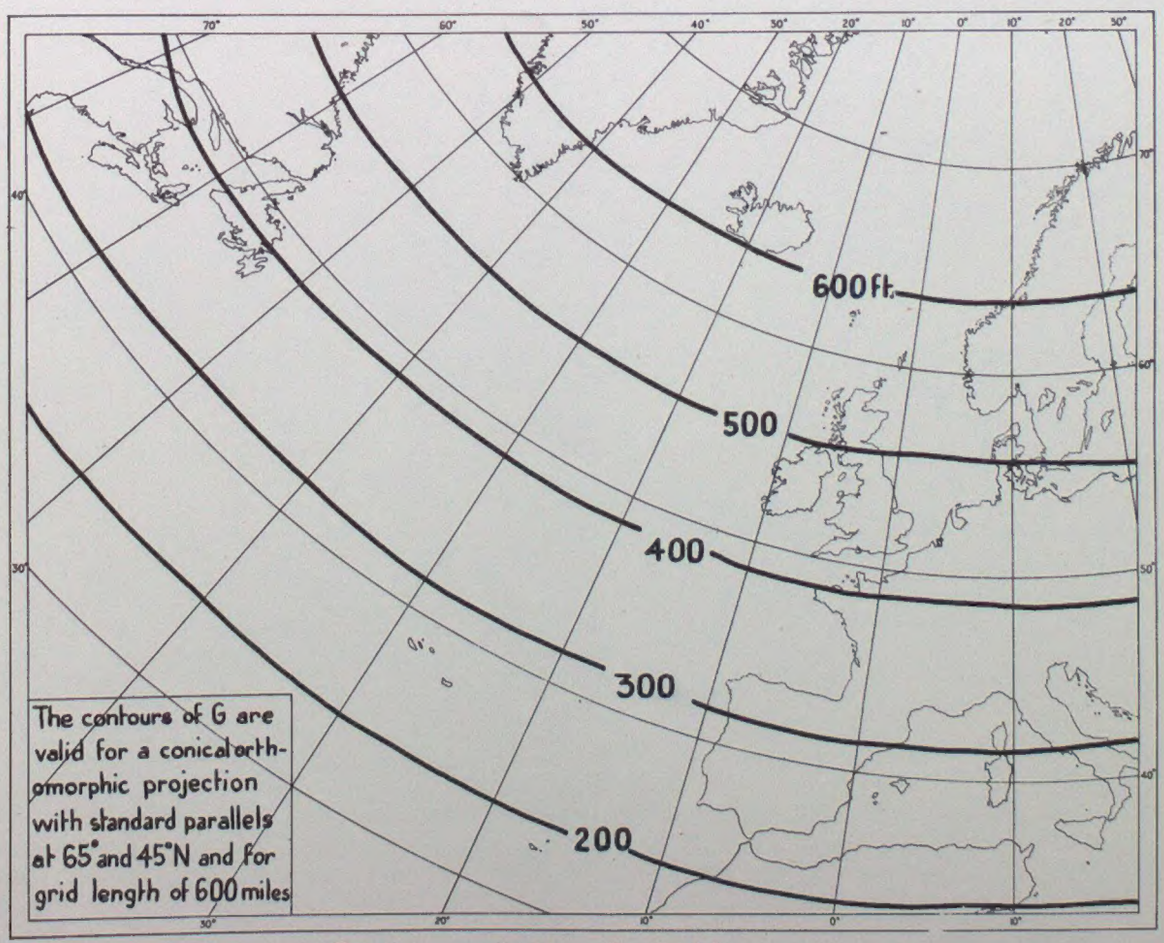

Fig.1. Contours of the G field

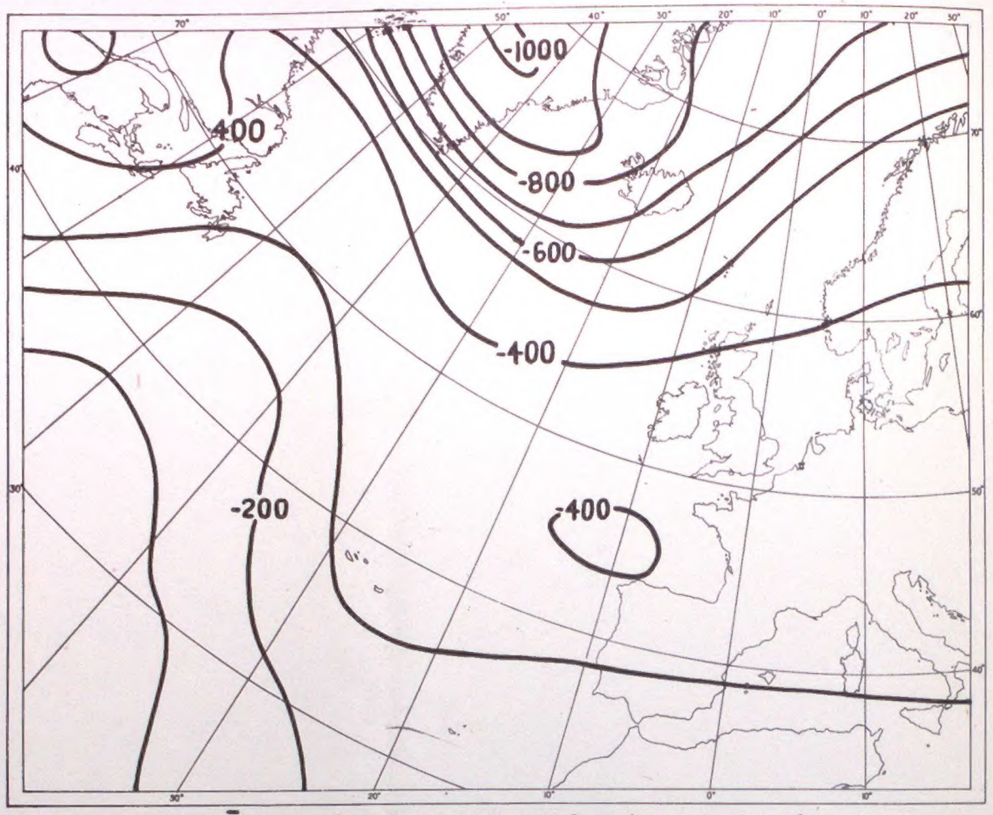

Fig.4. Original Z-$\bar{Z}$-G field 1500 G.M.T. 5:2:54 Units: ft.

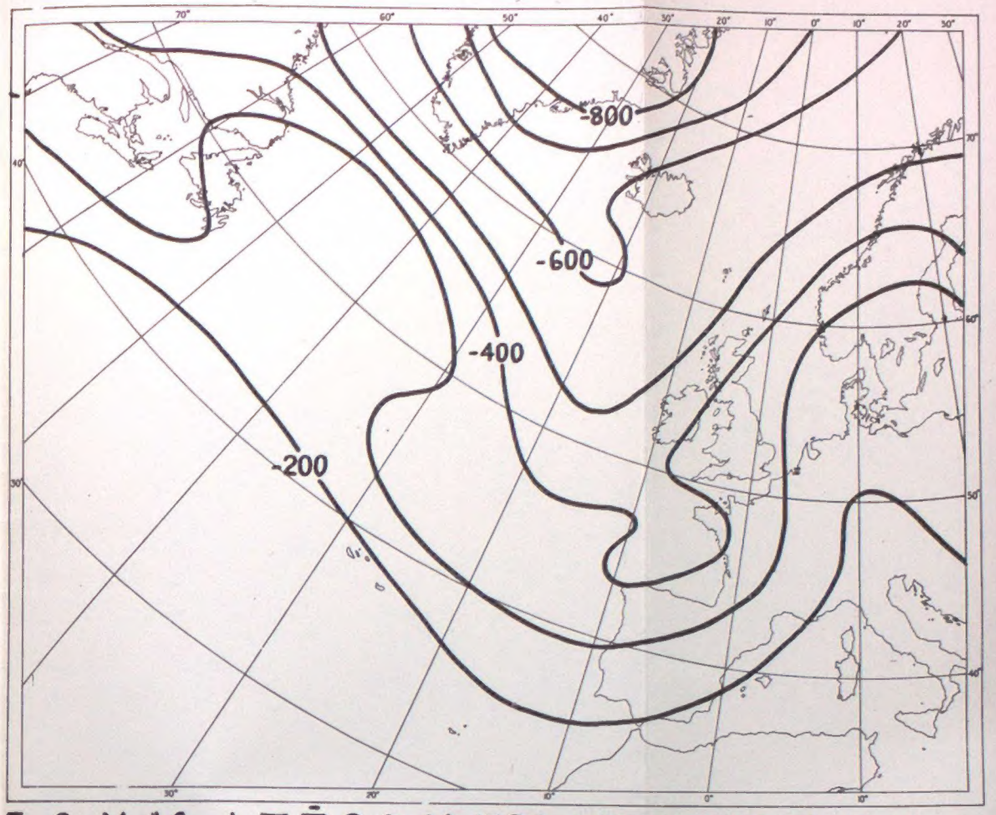

Fig.6. Modified Z-$\bar{Z}$-G field 1500 G.M.T. 5:2:54 Units: ft.

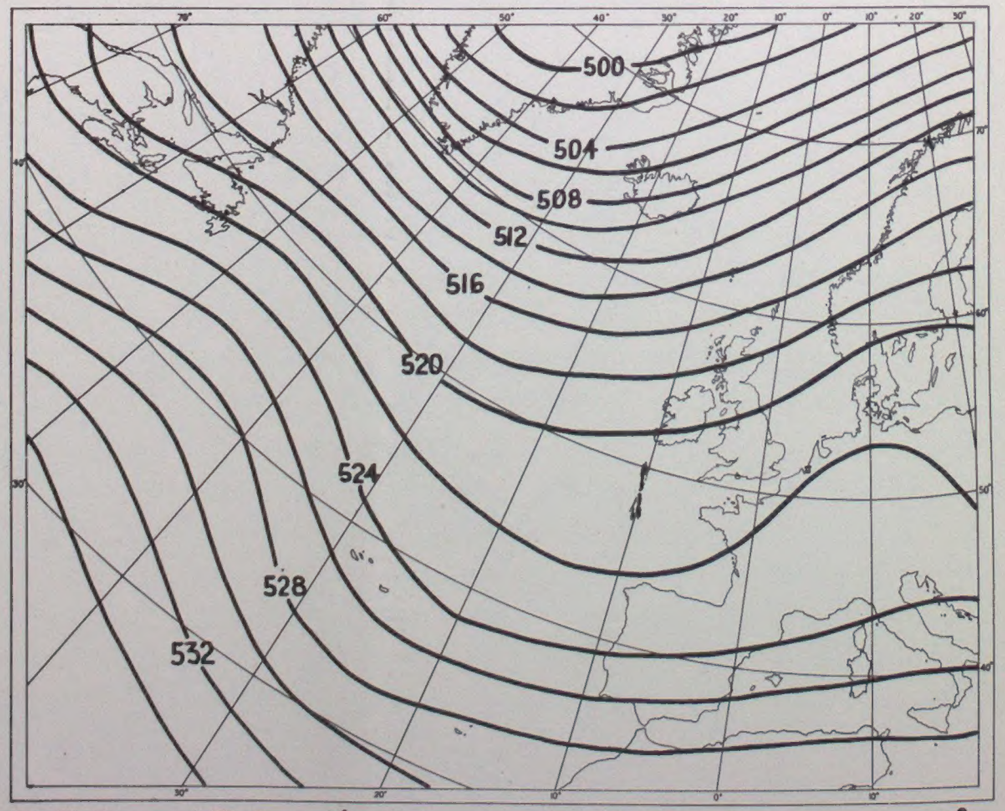

Fig.3. Original Z field (100 mb. contours) 1500 G.M.T. 5:2:54 Units 10^2 ft.

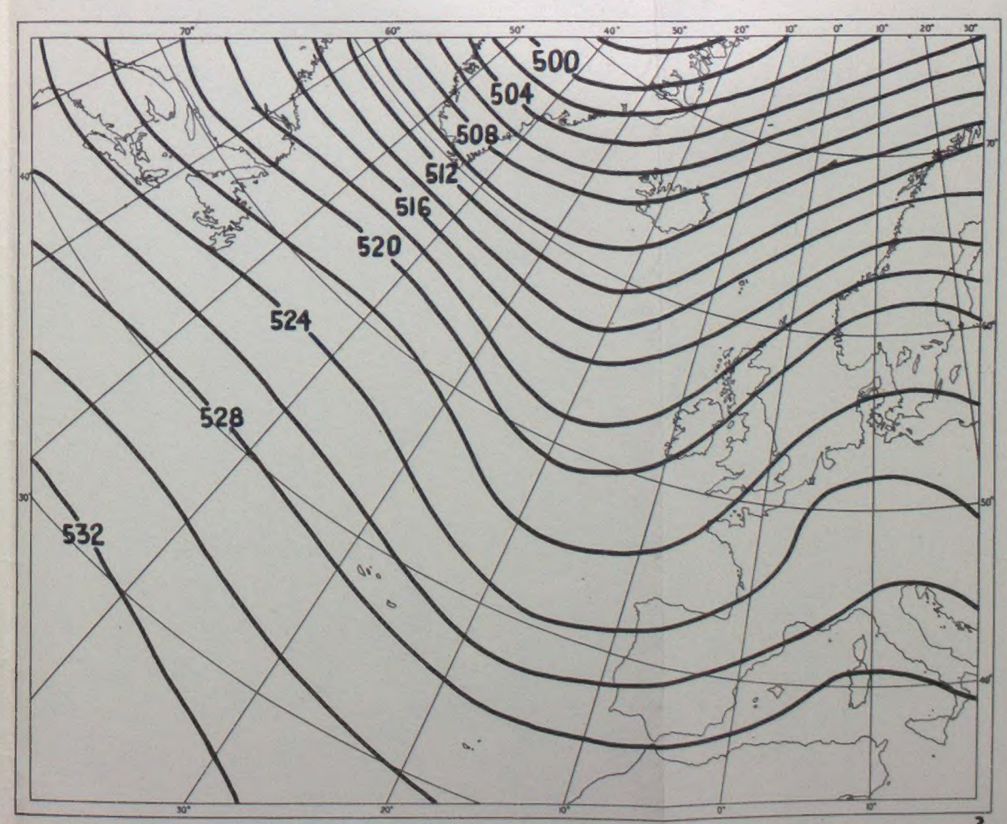

Fig.5. Modified Z field (100 mb. contours) 1500 G.M.T. 5:2:54 Units: 10^2 ft.

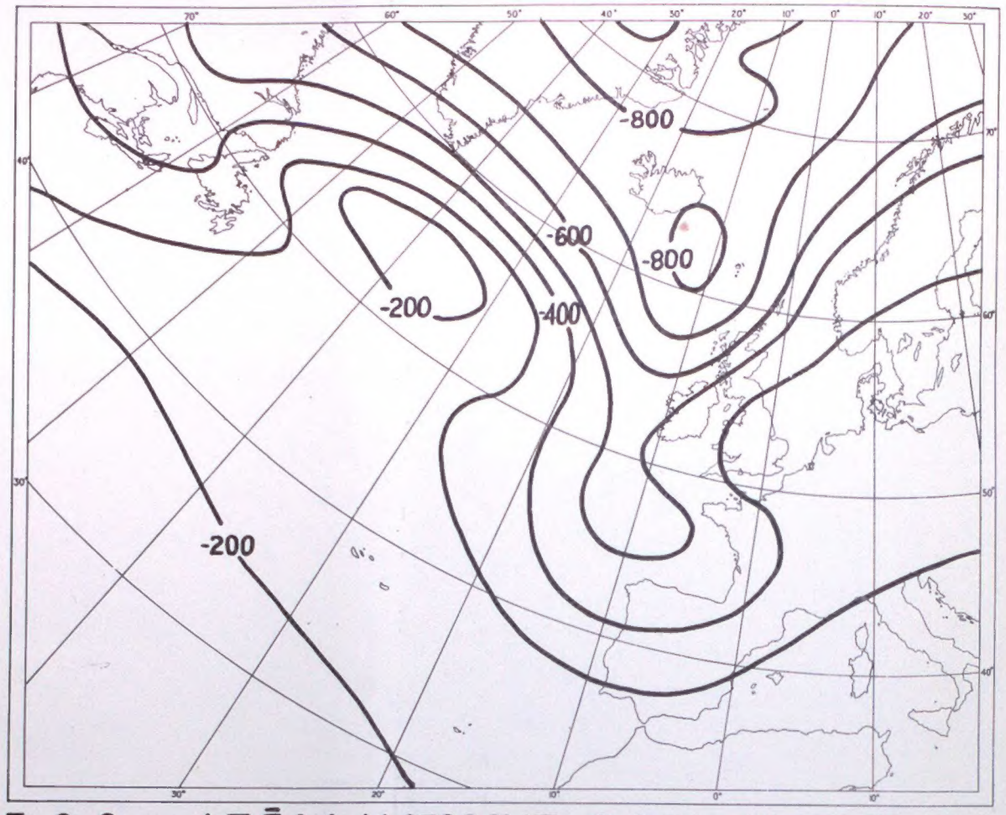

Fig.8. Original Z-$\bar{Z}$-G field 0300 G.M.T. 6:2:54 Units : ft.

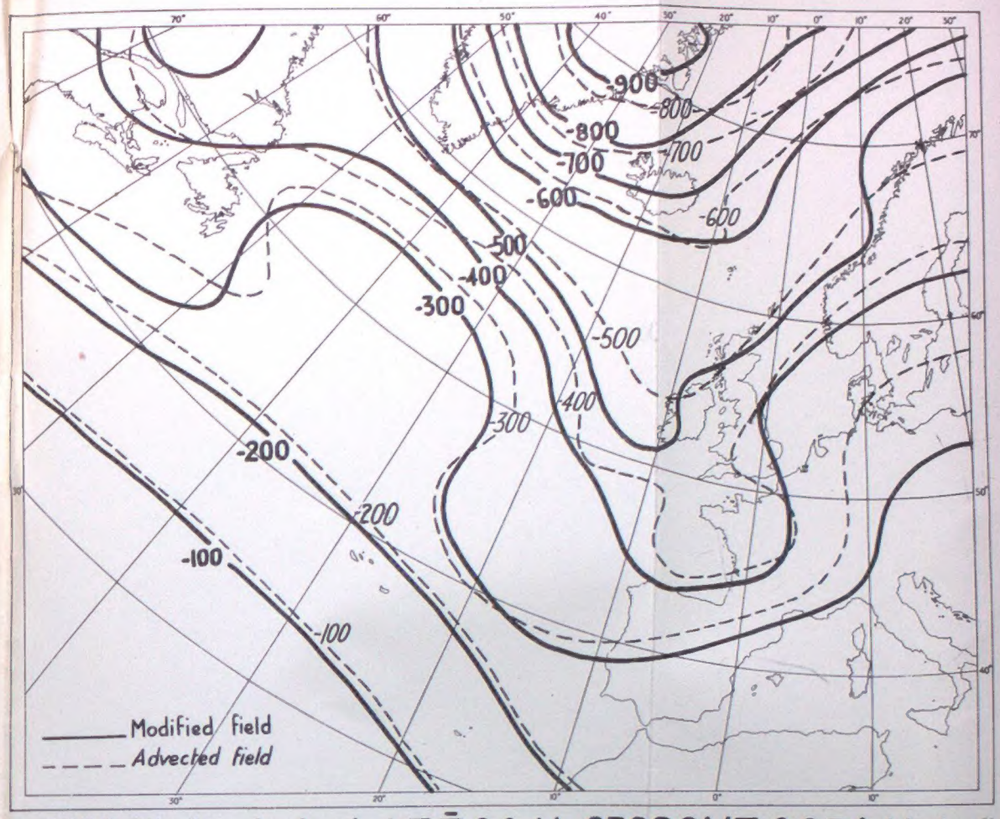

Fig.10. Modified and advected Z-$\bar{Z}$-G fields 0300 G.M.T. 6:2:54 Units: ft.

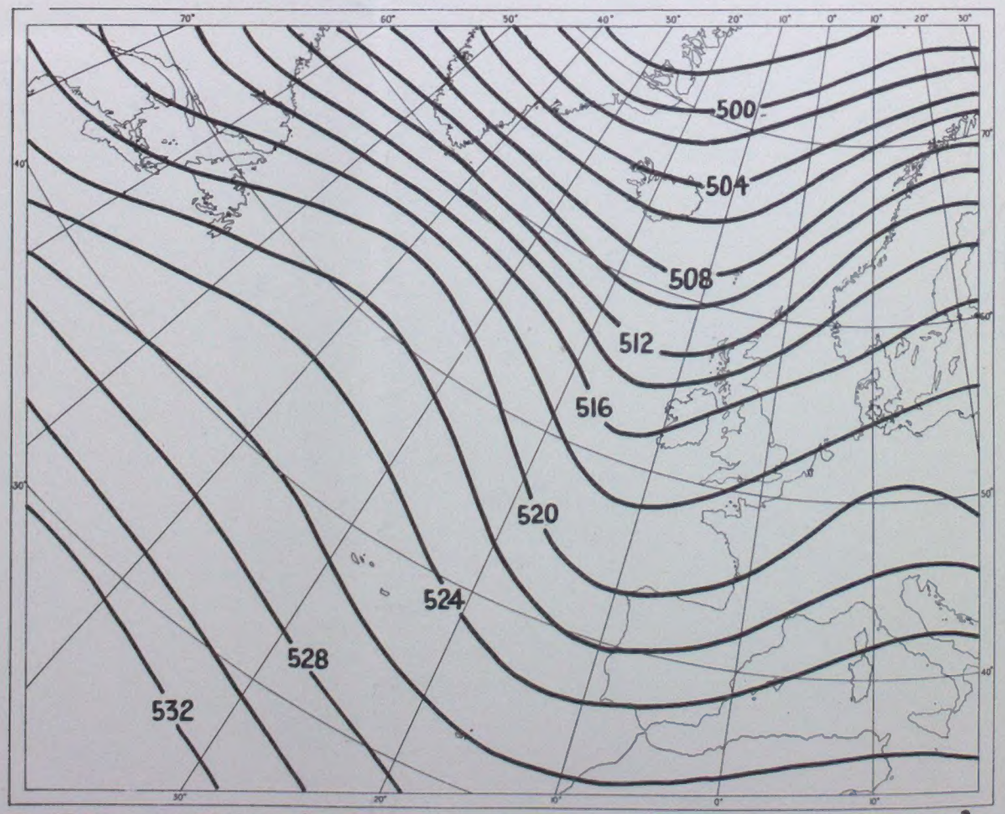

Fig.7. Original Z field (100 mb. contours) 0300 G.M.T. 6:2:54 Units 10^2 ft.

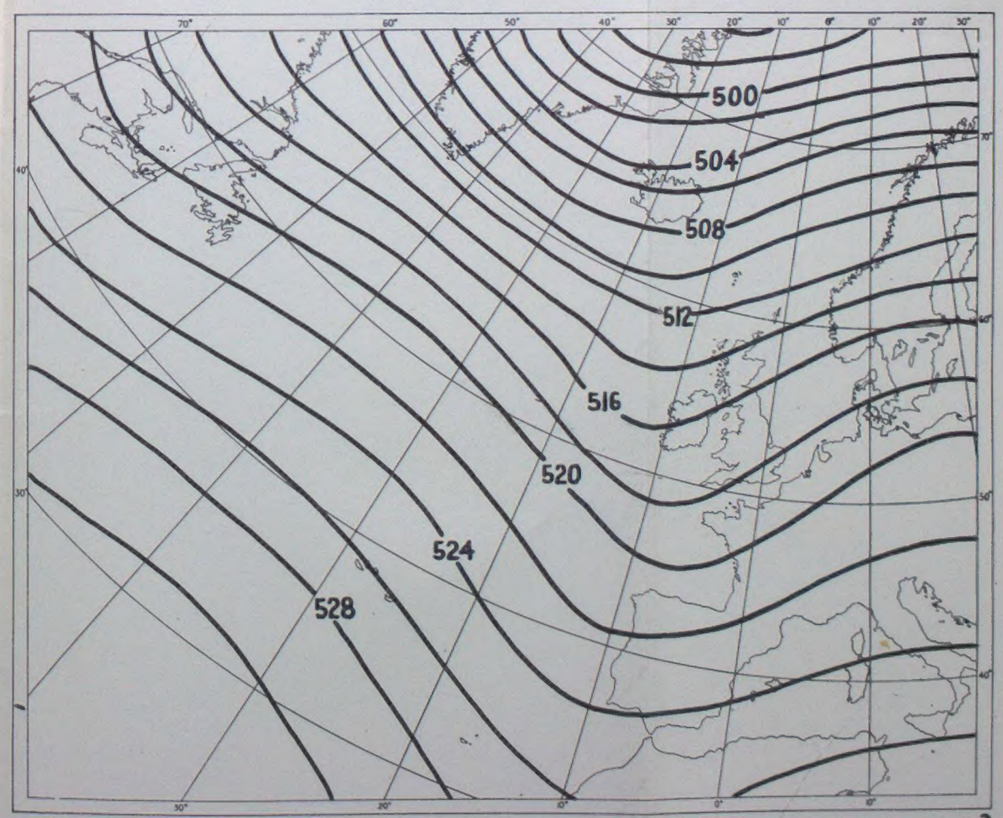

Fig. 9. Modified Z field (100 mb. contours) 0300 G.M.T. 6:2:54 Units: 10^2 ft.

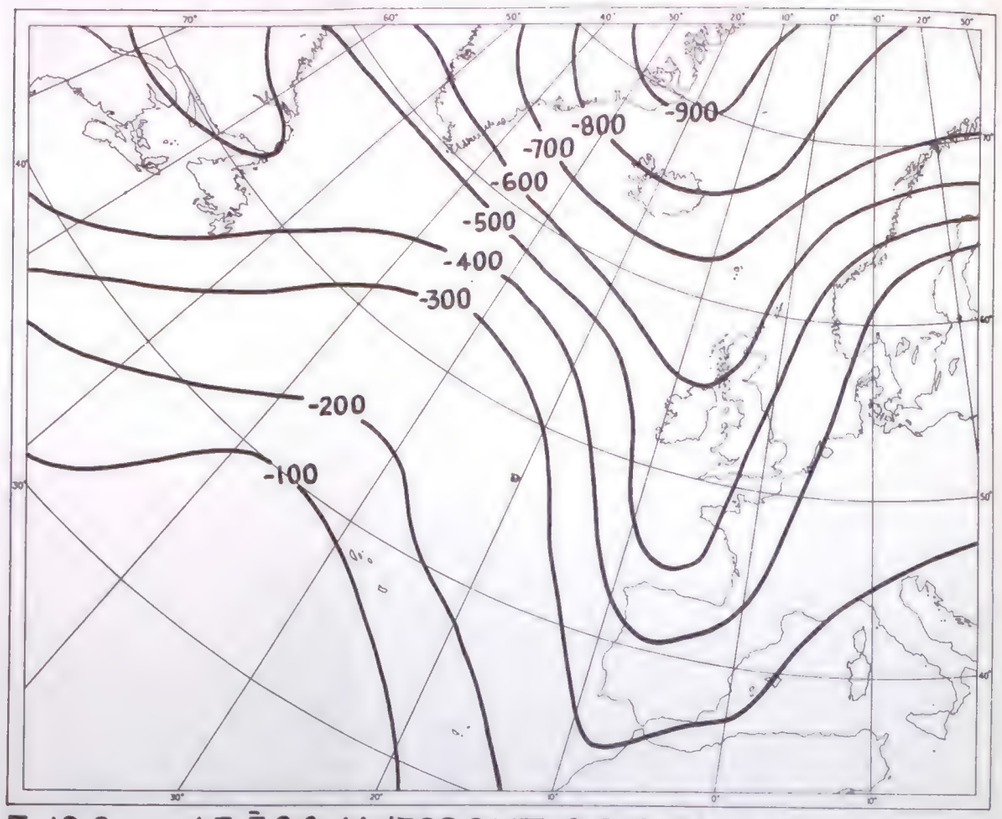

Fig12. Original Z-Z̄-G field 1500 G.M.T. 6:2:54 Units: Ft

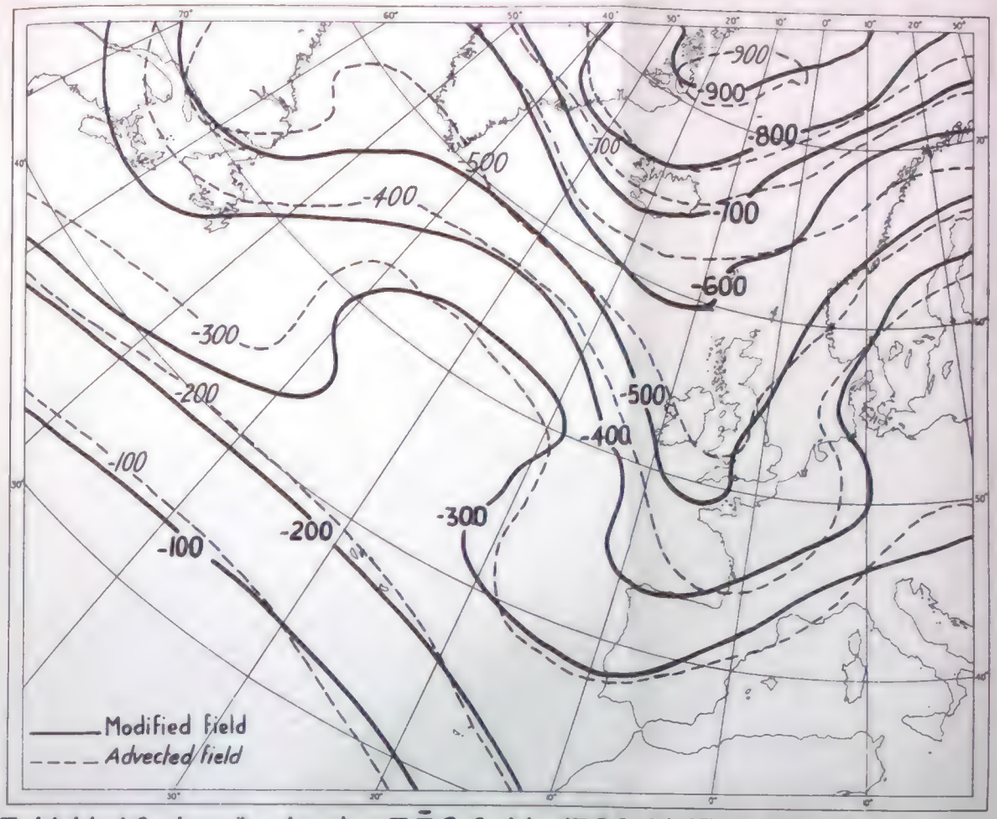

Fig14. Modified and advective Z-Z̄-G fields 1500 G.M.T. 6:2:54 Units: Ft

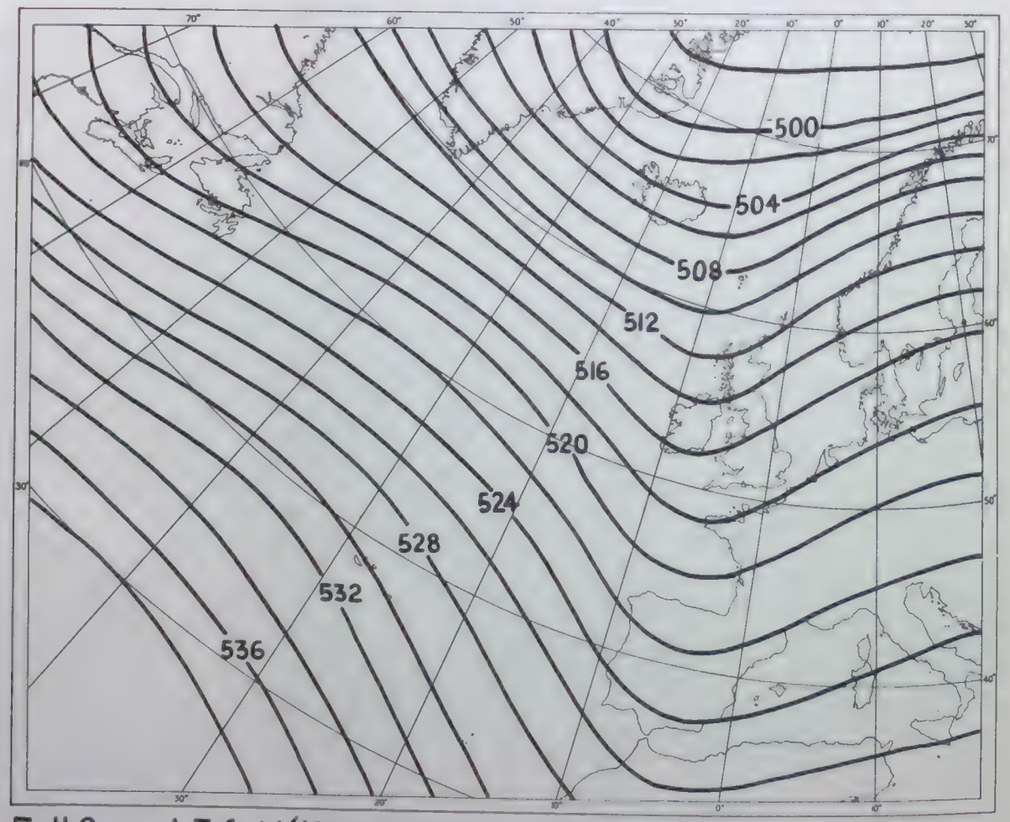

Fig11. Original Z field (100 mb. contours) 1500 G.M.T. 6:2:54 Units: 10^2 Ft.

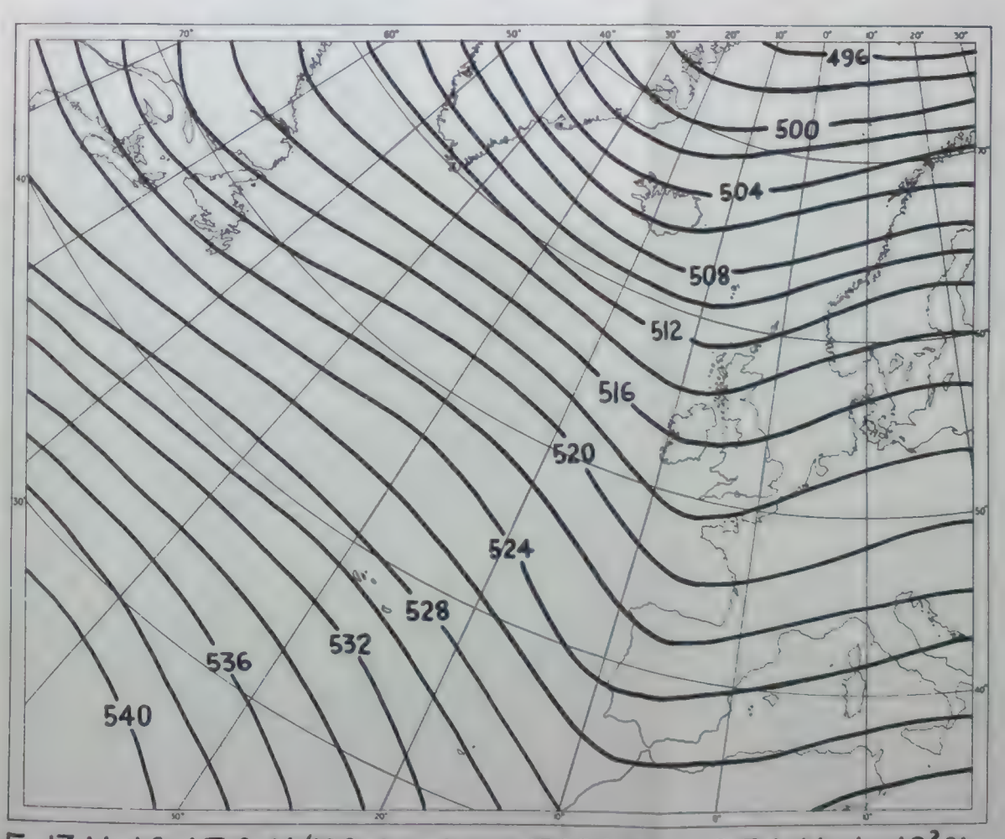

Fig13. Modified Z field (100 mb. contours) 1500 G.M.T. 6:2:54 Units 10^2 Ft.

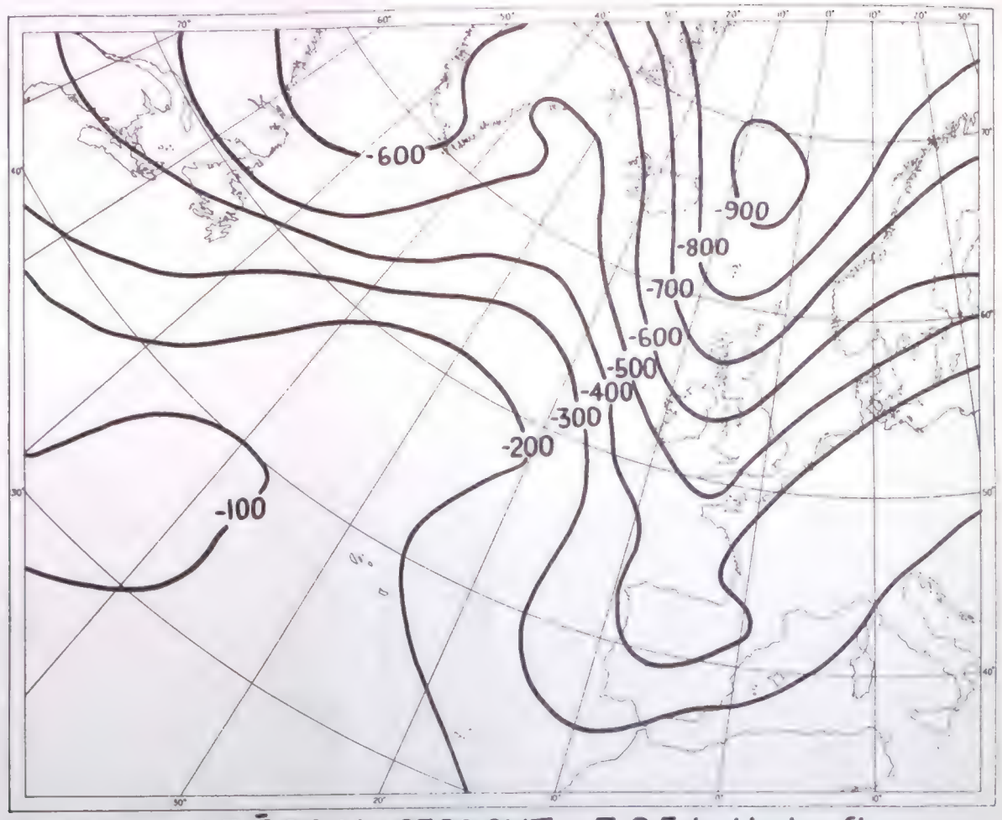

Fig. 16. Original Z-Z̄-6 fields 0300 G.M.T. 7:2:54 Units: Ft.

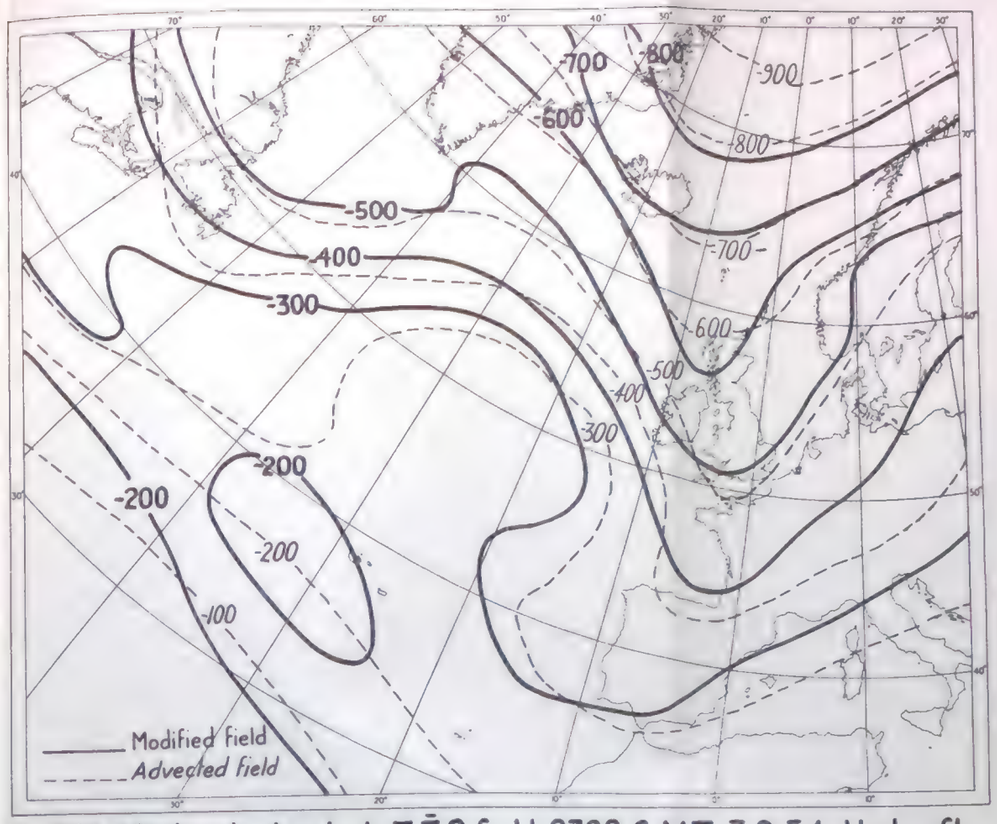

Fig. 18. Modified and advected Z-Z̄-G field 0300 G.M.T. 7:2:54 Units: Ft.

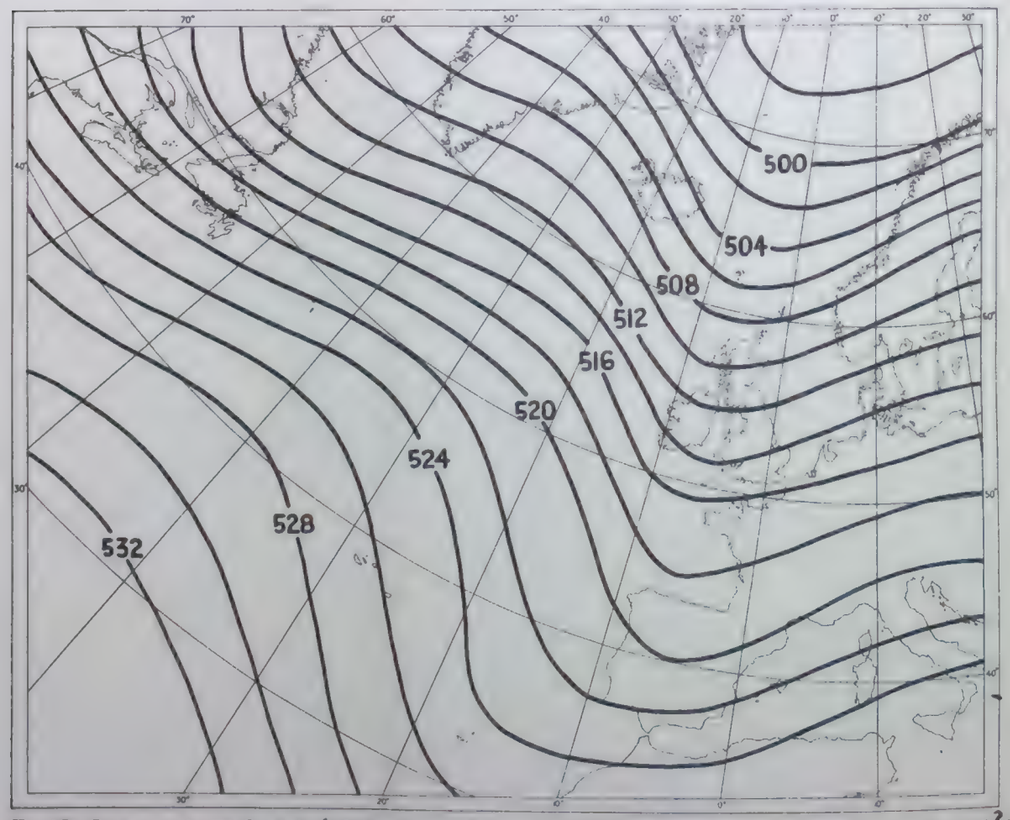

Fig. 15. Original Z field (100 mb. contours) 0300 G.M.T. 7:2:54 Units: 10^2 ft.

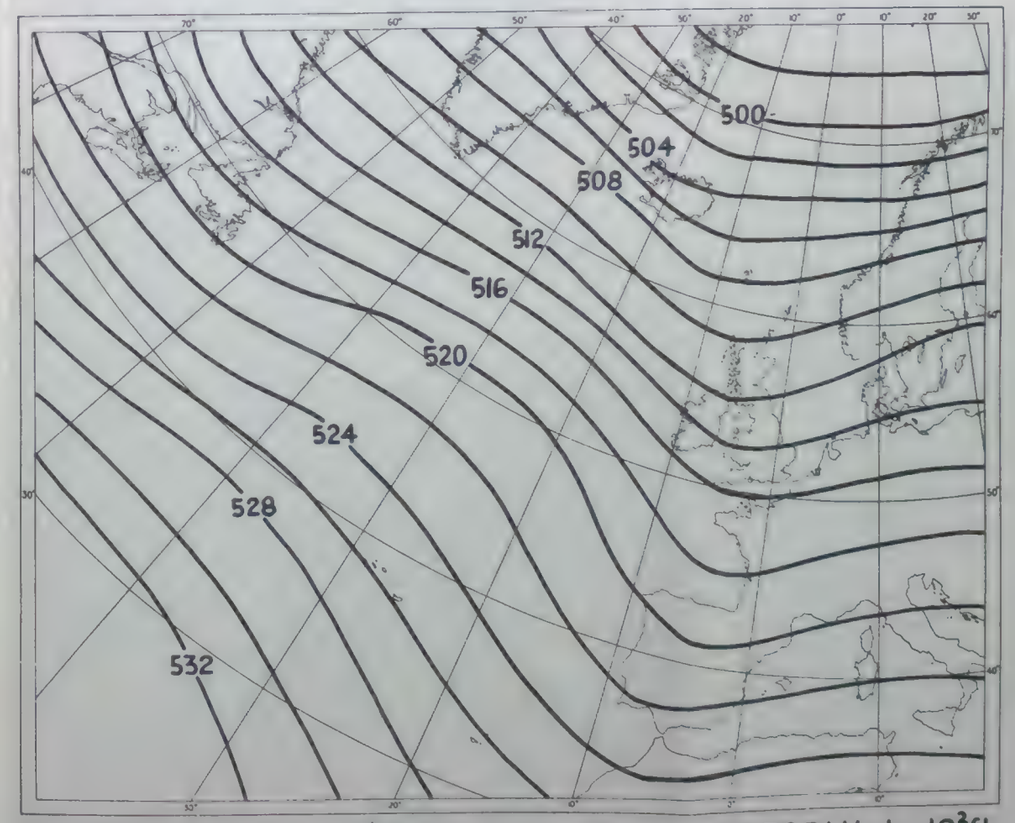

Fig. 17. Modified Z field (100 mb. contours) 0300 G.M.T. 7:2:54 Units: 10^2 ft.

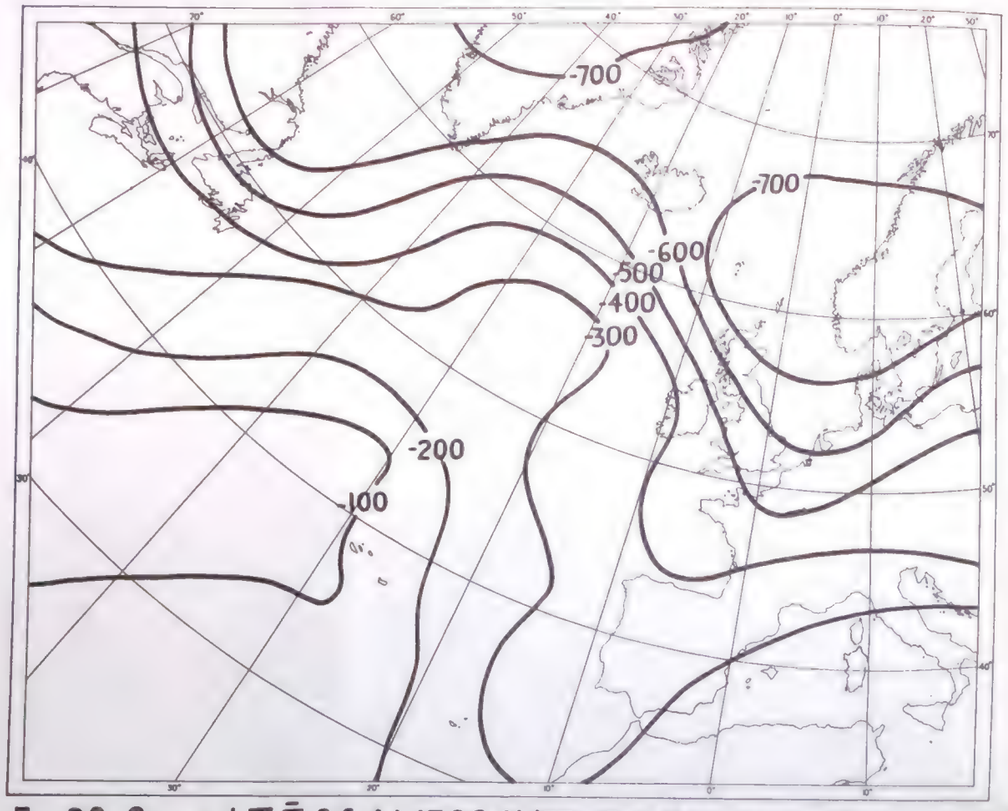

Fig.20. Original Z-$\bar{Z}$-G field 1500 G.M.T. 7:2:54 Units: ft.

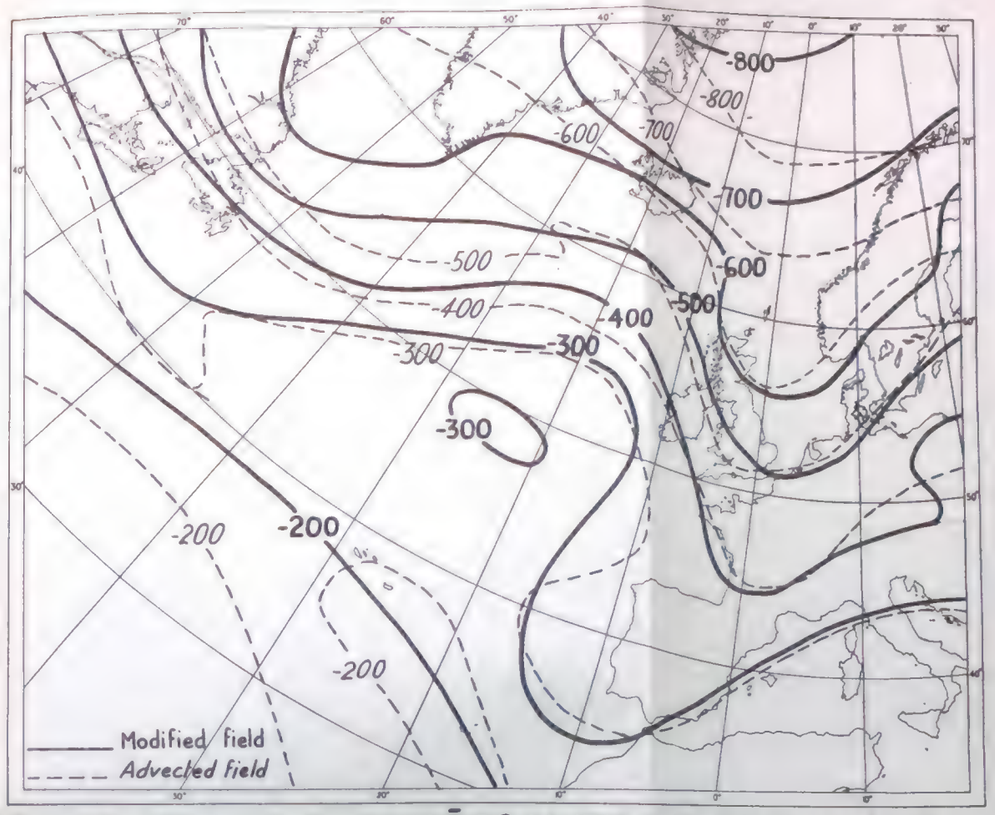

Fig.22. Modified and advected Z-$\bar{Z}$-G fields 1500 G.M.T. 7:2:54 Units: ft.

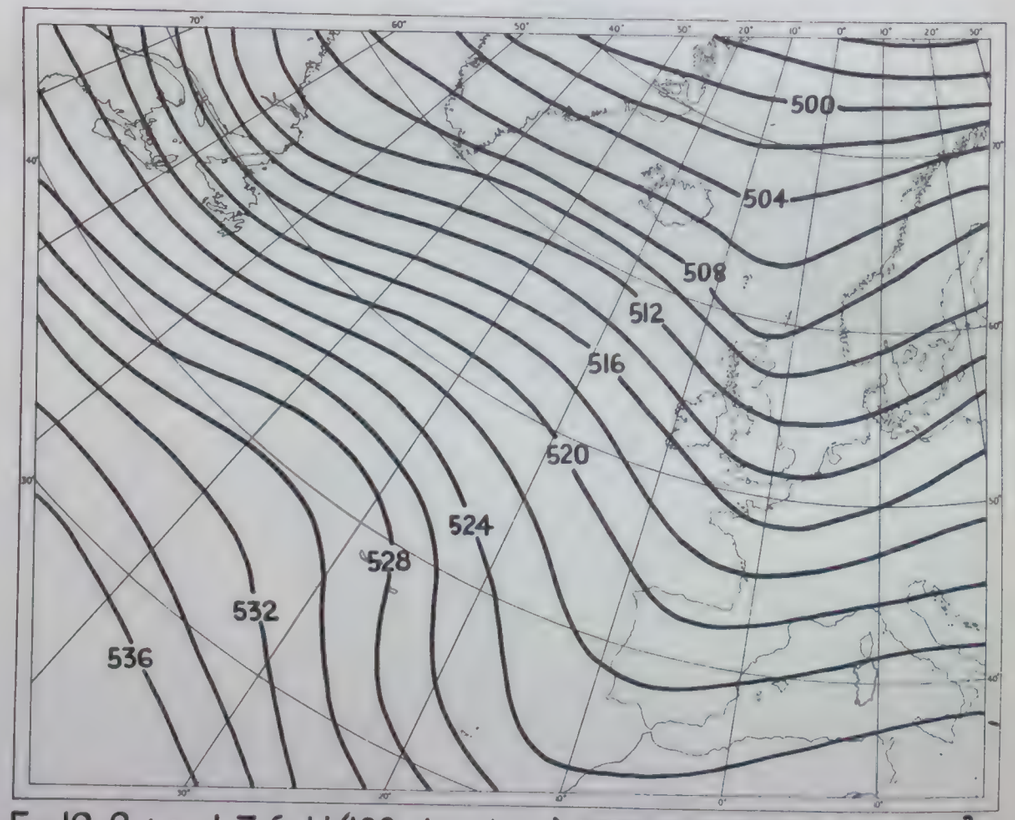

Fig.19. Original Z field (100 mb. contours) 1500 G.M.T. 7:2:54 Units: 10^2 ft.

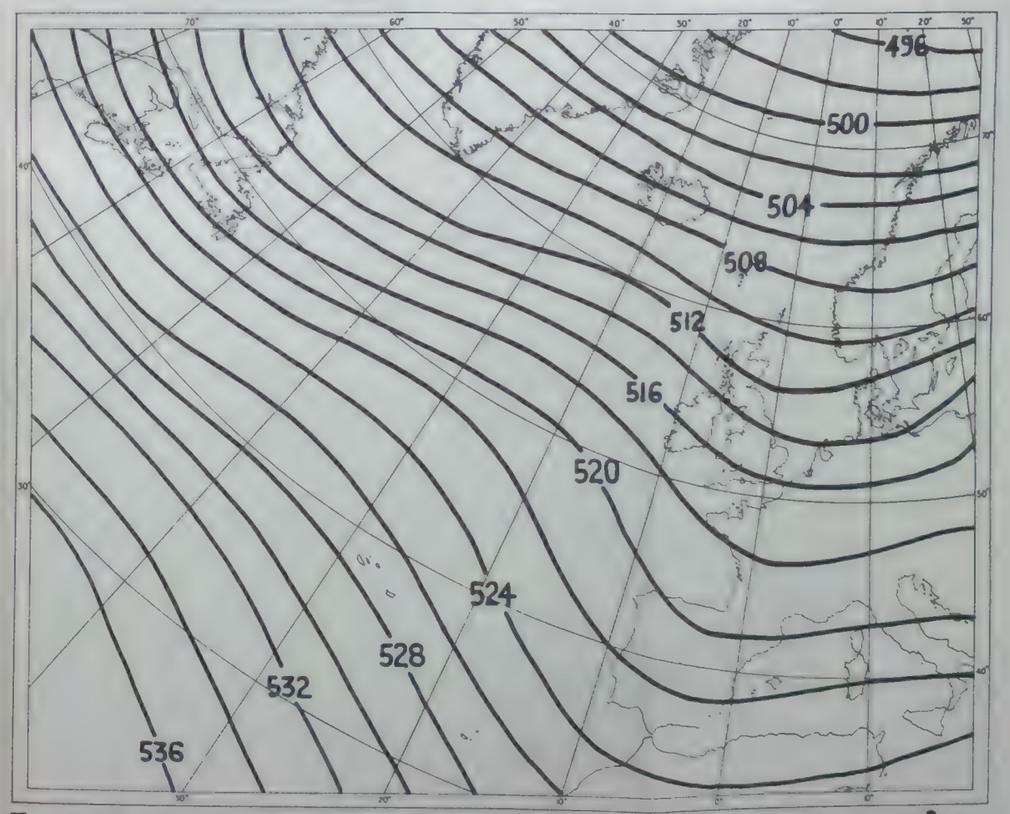

Fig.21. Modified Z field (100 mb. contours) 1500 G.M.T. 7:2:54 Units 10^2 ft.

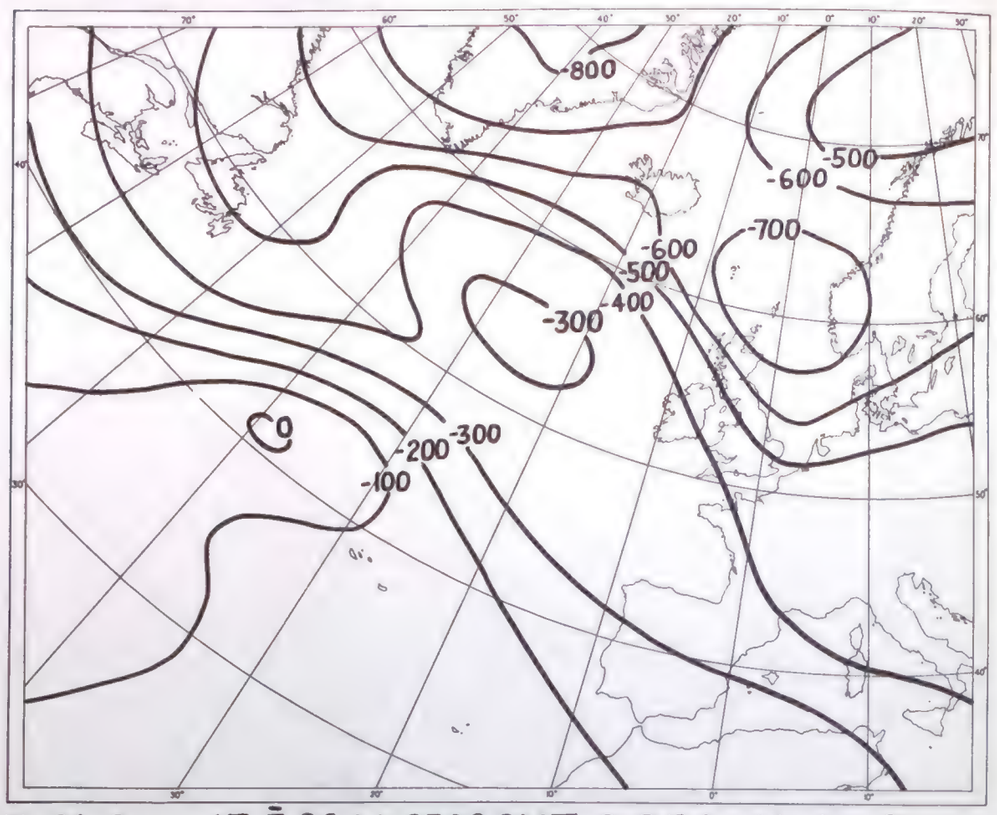

Fig.24. Original Z-$\bar{Z}$-G field 0300 G.M.T. 8:2:54 Units: ft.

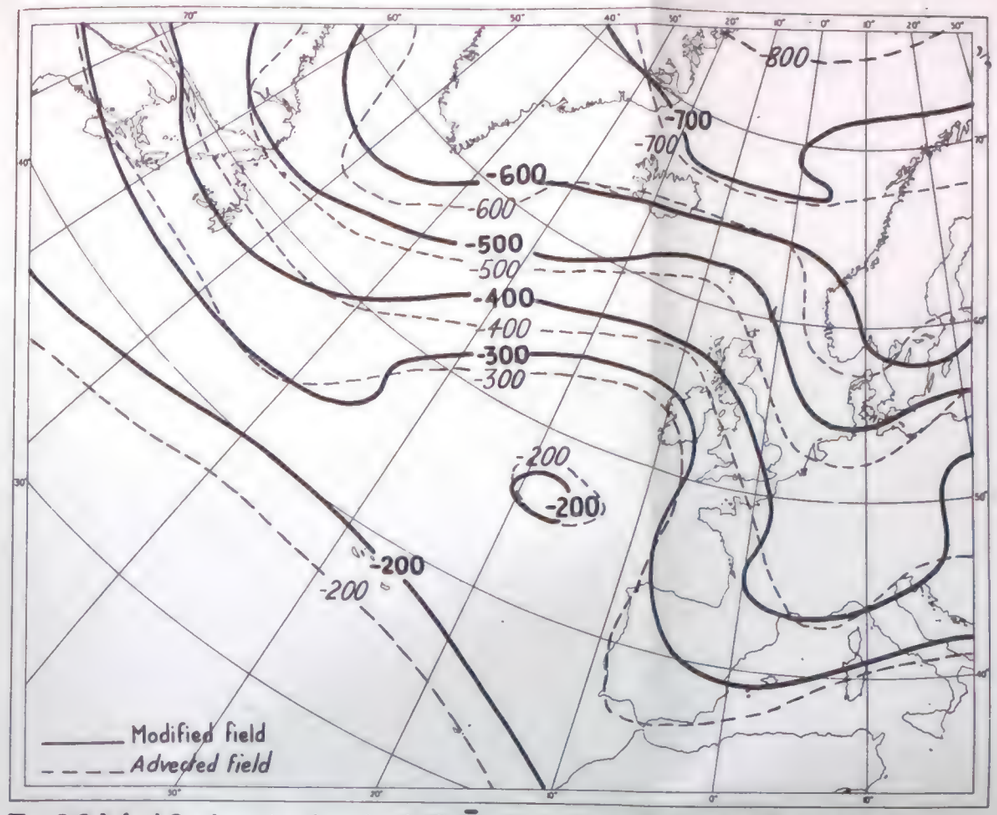

Fig.26. Modified and advected Z-$\bar{Z}$-G fields 0300 G.M.T. 8:2:54 Units ft.

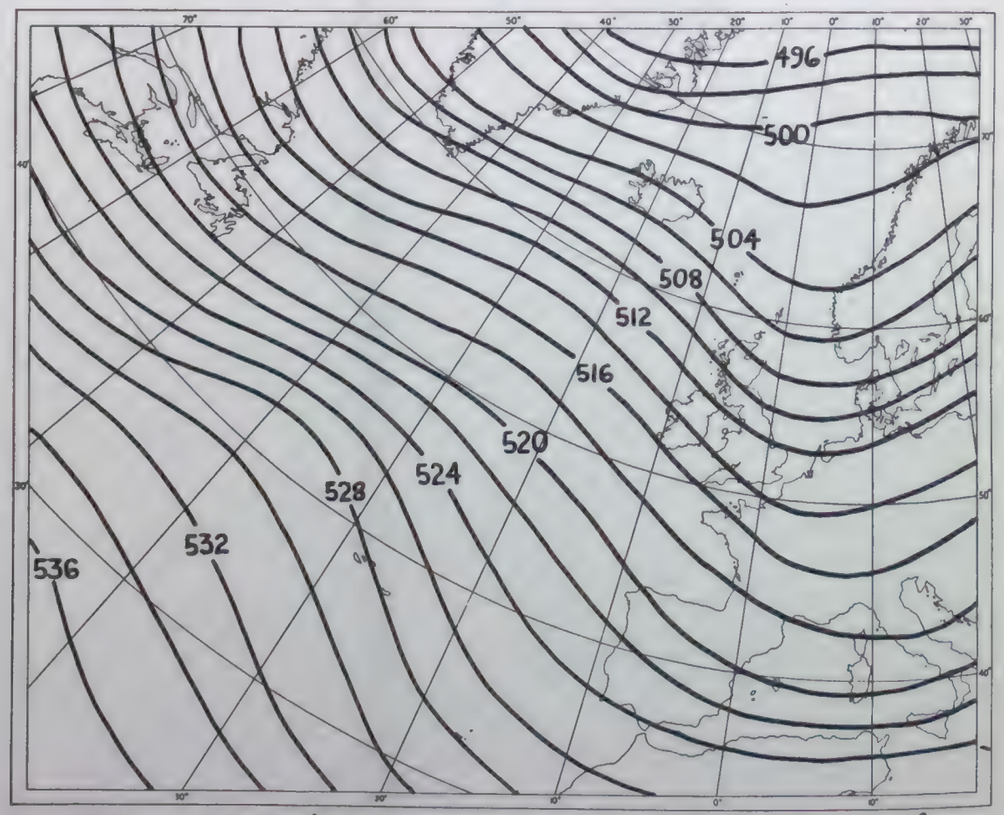

Fig.23. Original Z field (100mb. contours) 0300 G.M.T. 8:2:54 Units: 10^2 ft.

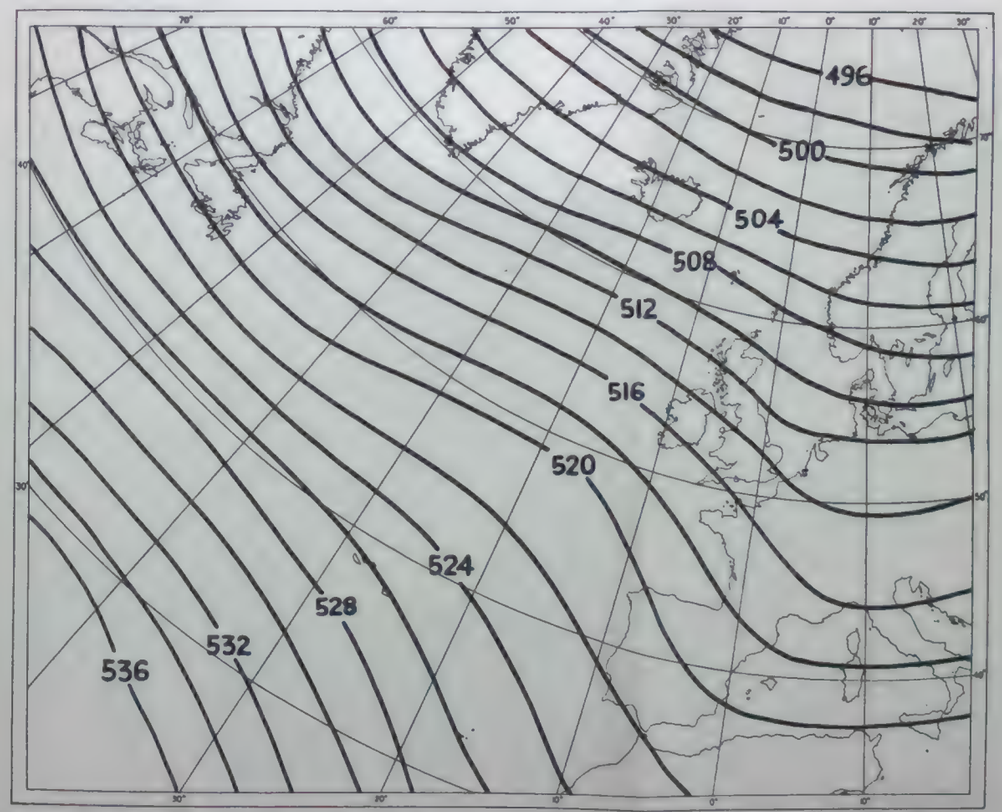

Fig.25. Modified Z field (100mb. contours) 0300 G.M.T. 8:2:54 Units 10^2 ft.

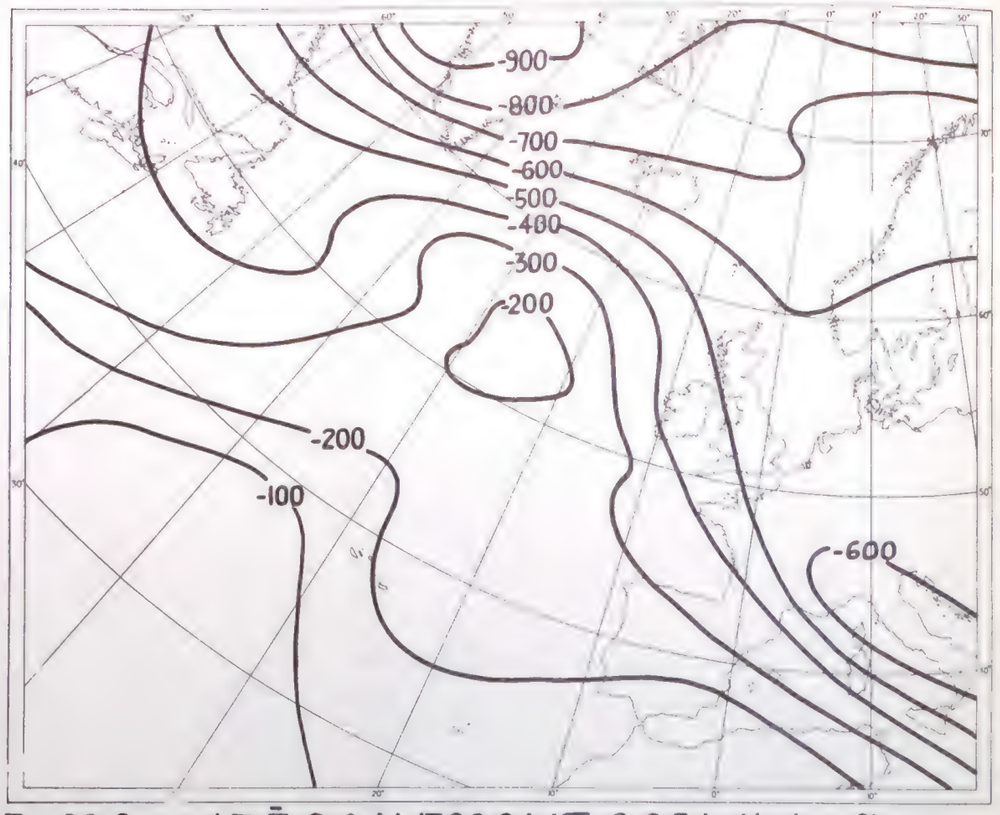

Fig. 28. Original Z-Ż-G field 1500 G.M.T. 8:2:54 Units: ft

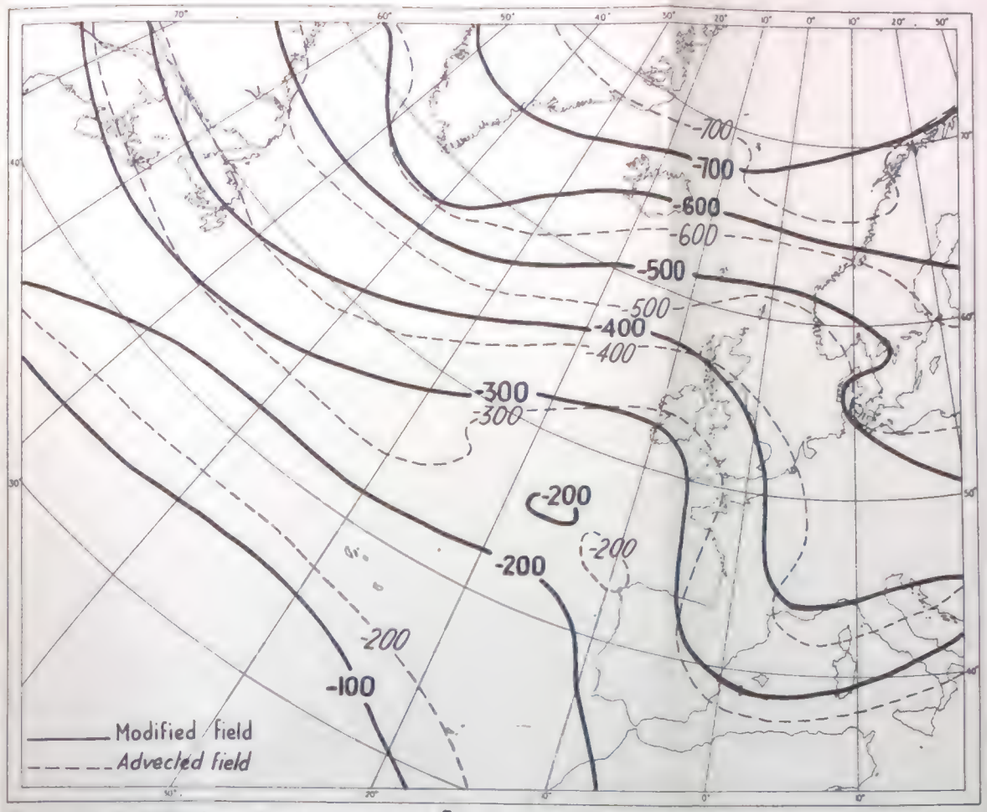

Fig. 30. Modified and advected Z-Ż-G fields 1500 G.M.T. 8:2:54 Units: ft

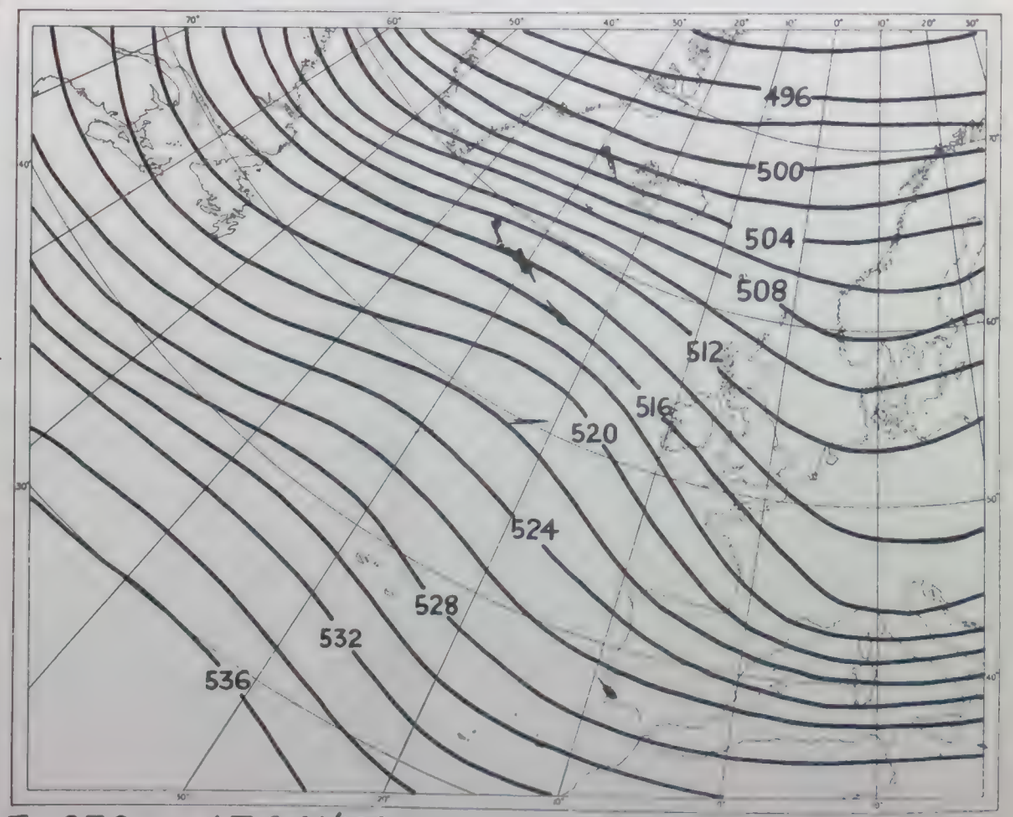

Fig. 27. Original Z field (100mb. contours) 1500 G.M.T. 8:2:54 Units 10^2 ft.

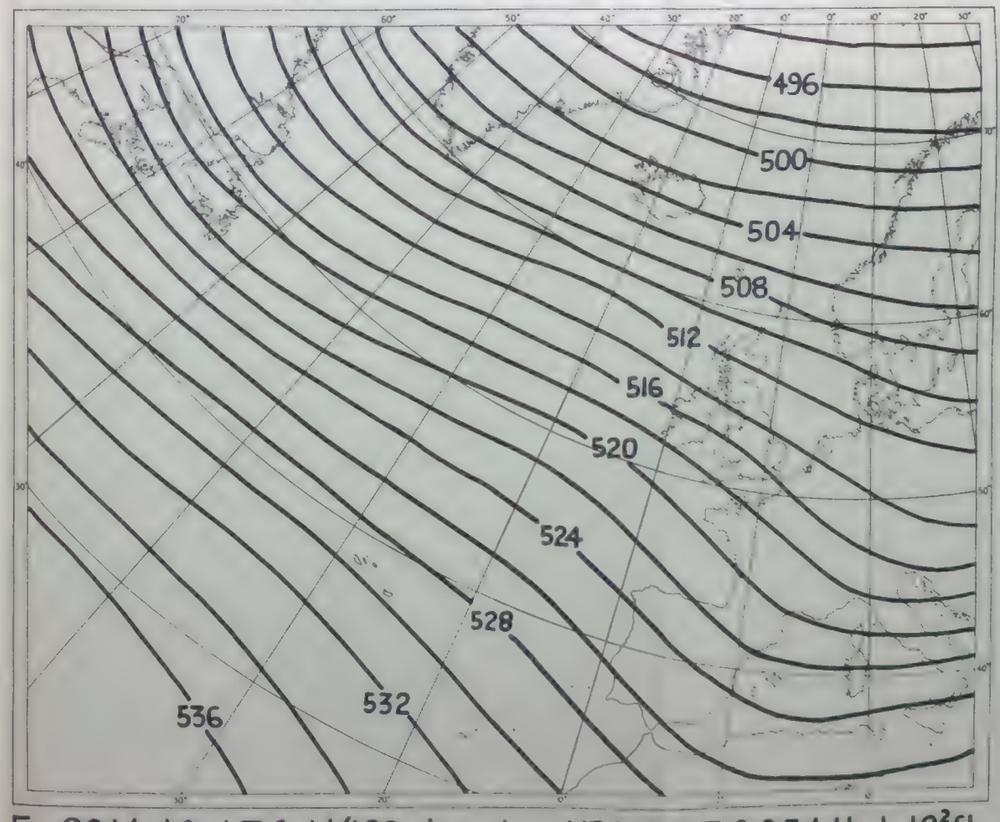

Fig. 29. Modified Z field (100mb. contours) 1500 G.M.T. 8:2:54 Units 10^2 ft.

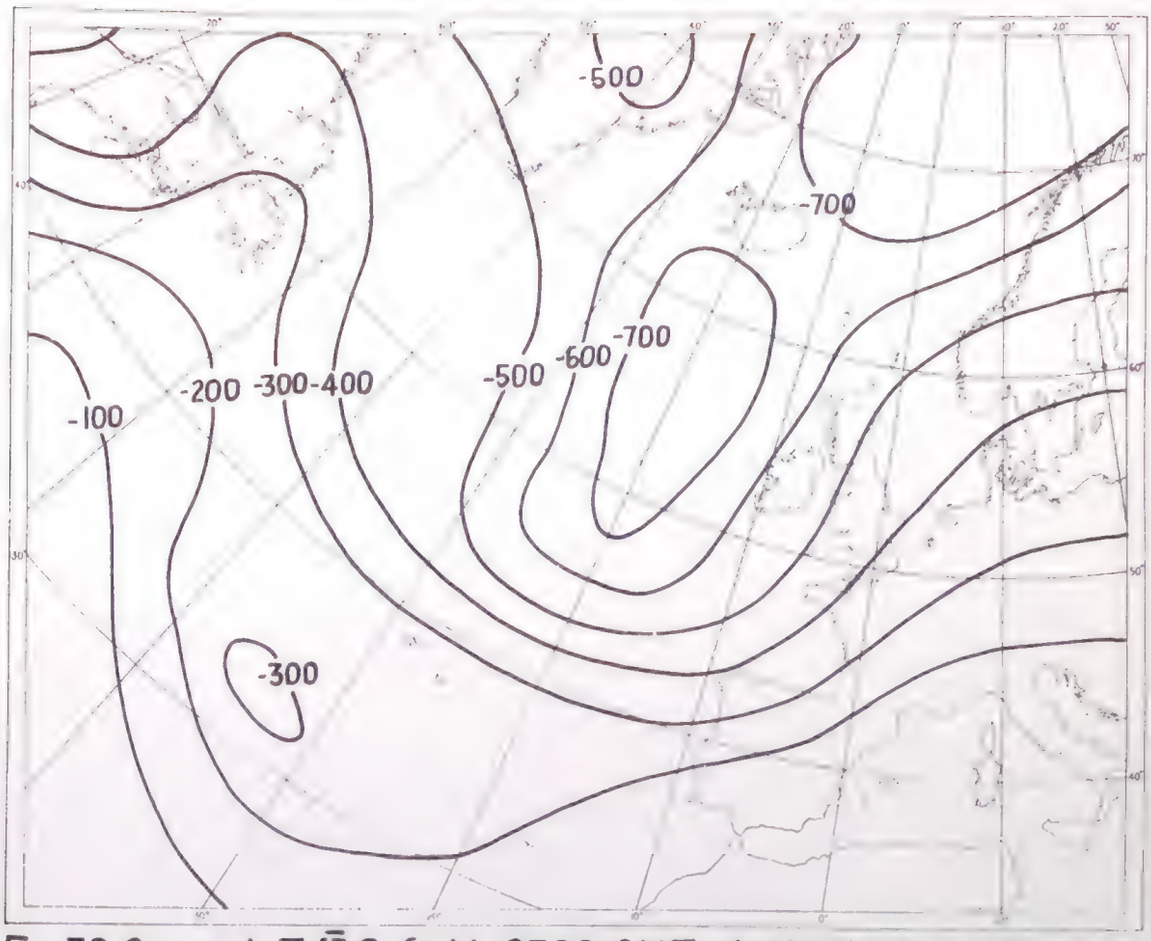

Fig.32. Original Z-$\bar{Z}$-G field 0300 G.M.T. 4:11:55 Units: Ft.

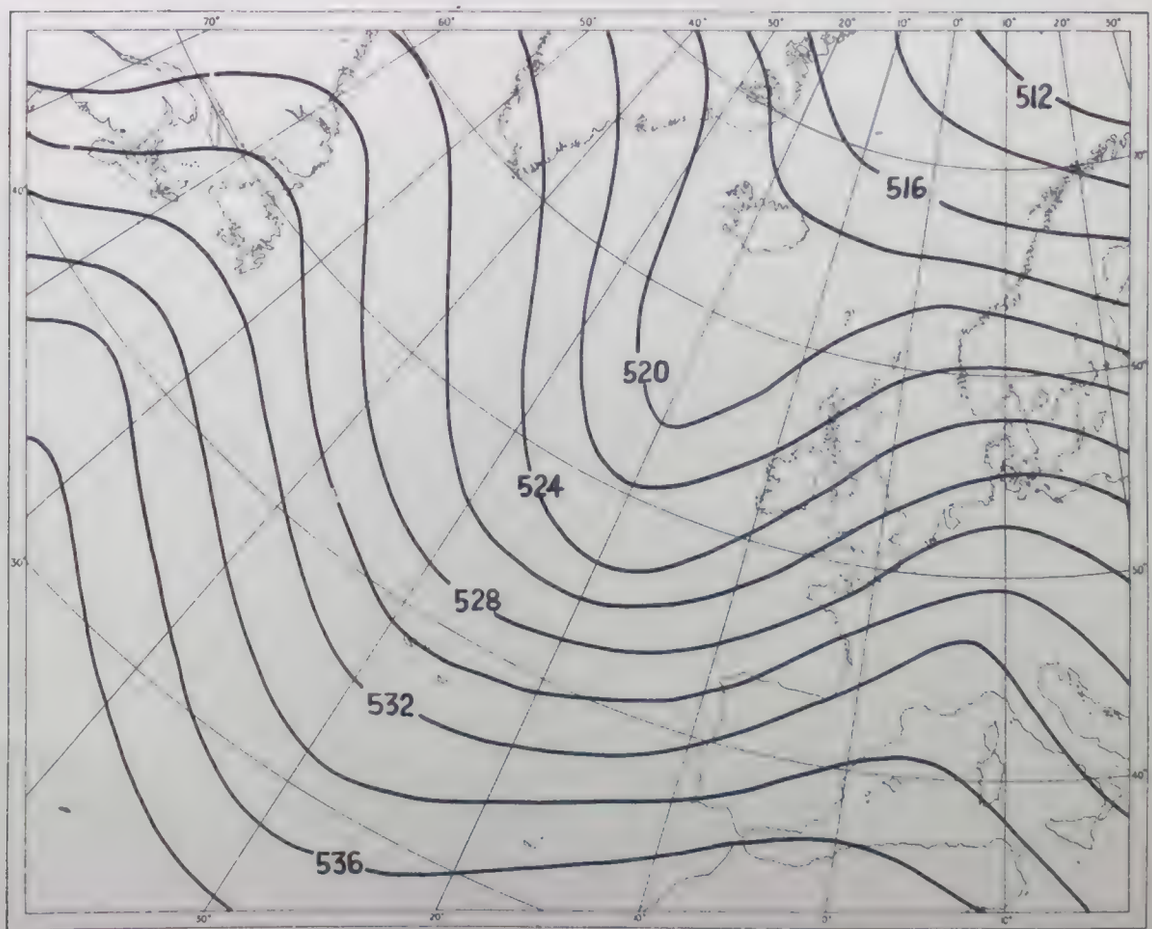

Fig.31. Original Z field (100 mb. contours) 0300 G.M.T. 4:11:55 Units: 10^2 ft.

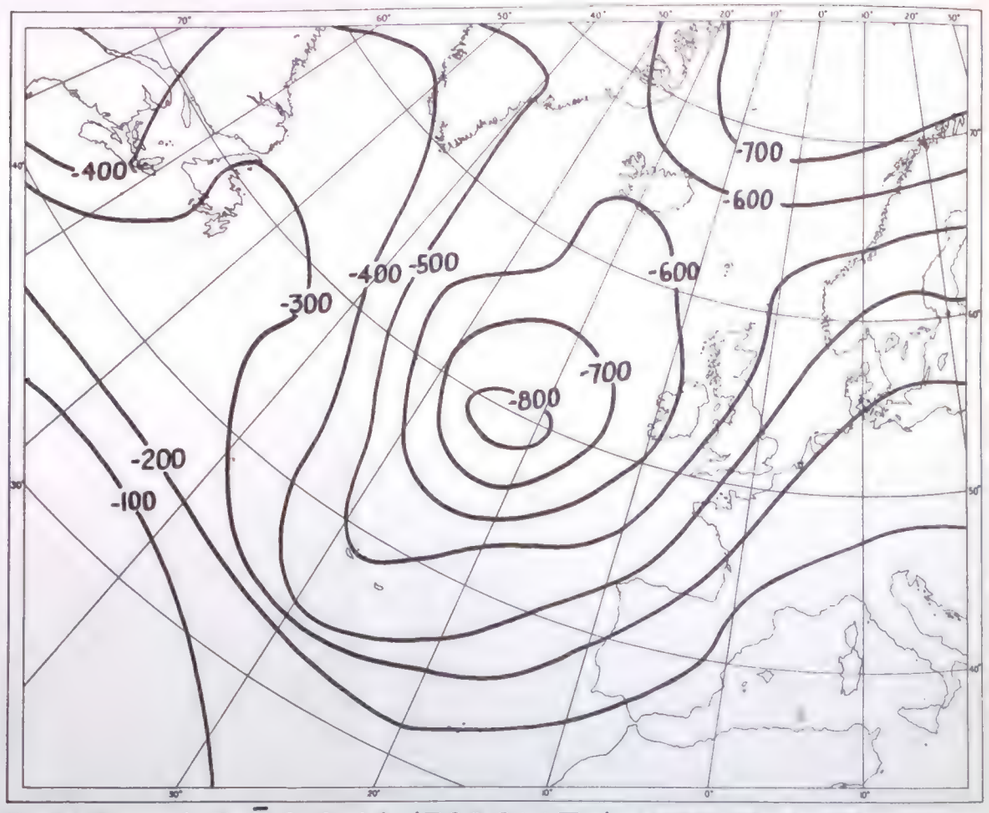

Fig.34. Original Z-$\bar{Z}$-G field 1500 G.M.T. 4:11:55 Units: ft

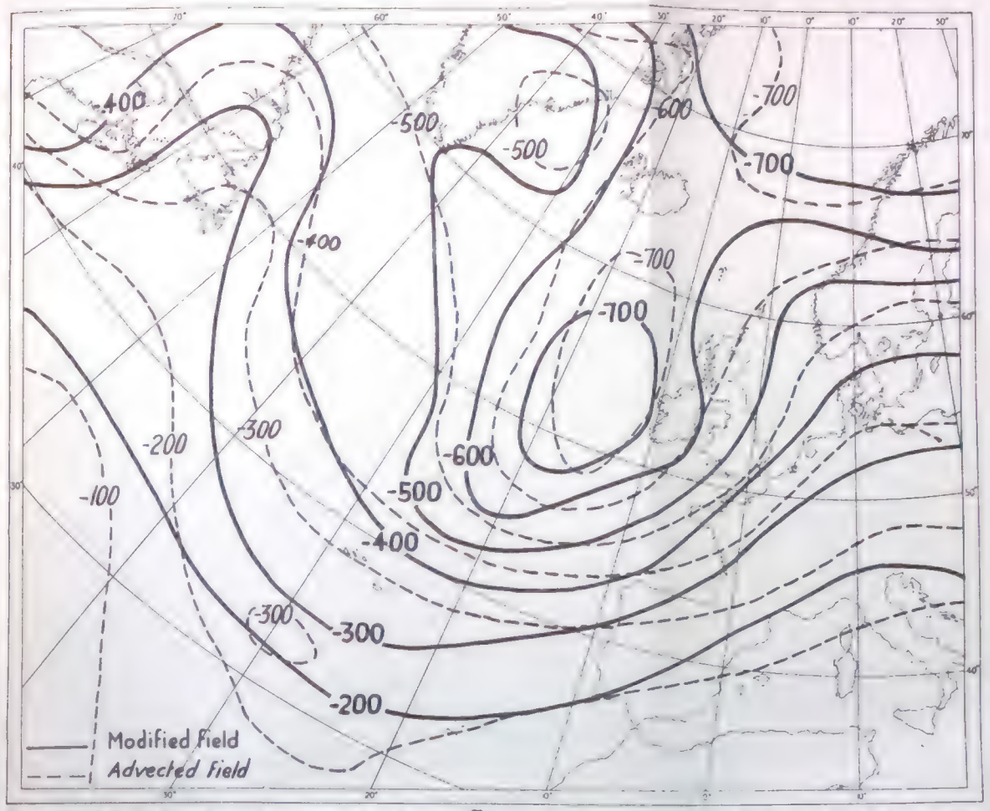

Fig.36. Modified and advected Z-$\bar{Z}$-G fields 1500 G.M.T. 4:11:55 Unit: ft

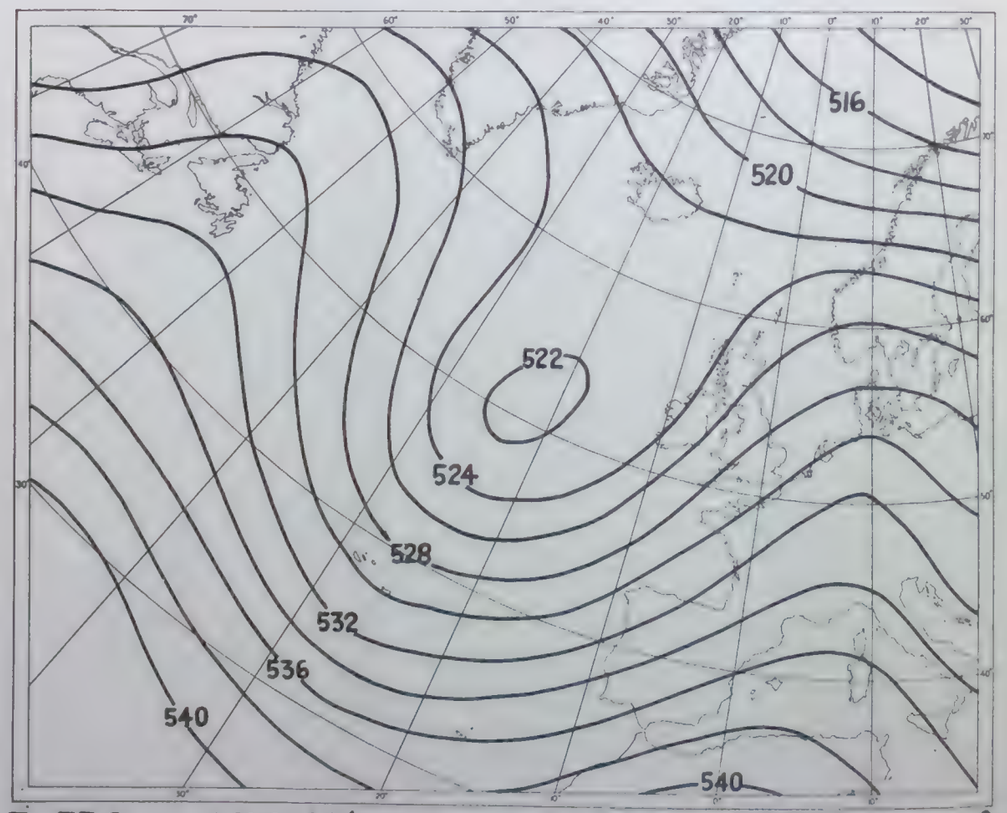

Fig.33. Original Z field (100mb contours) 1500 G.M.T. 4:11:55 Units: 10^2 ft.

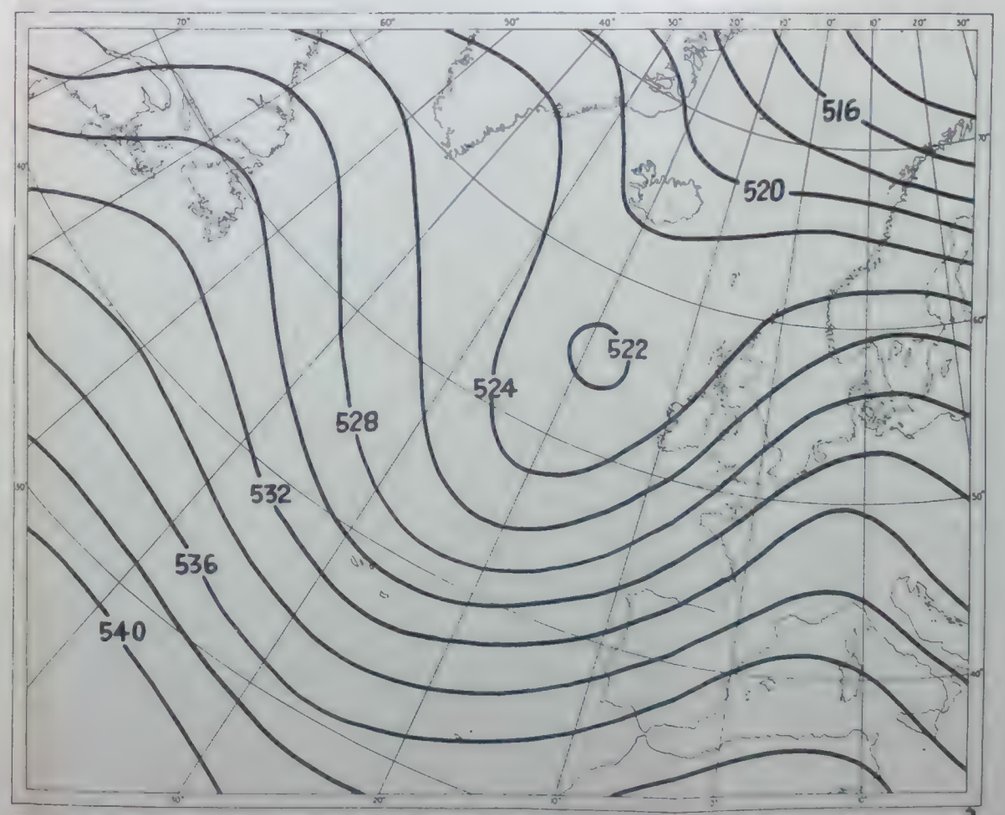

Fig.35. Modified Z field (100mb contours) 1500 G.M.T. 4:11:55 Units: 10^2 ft.

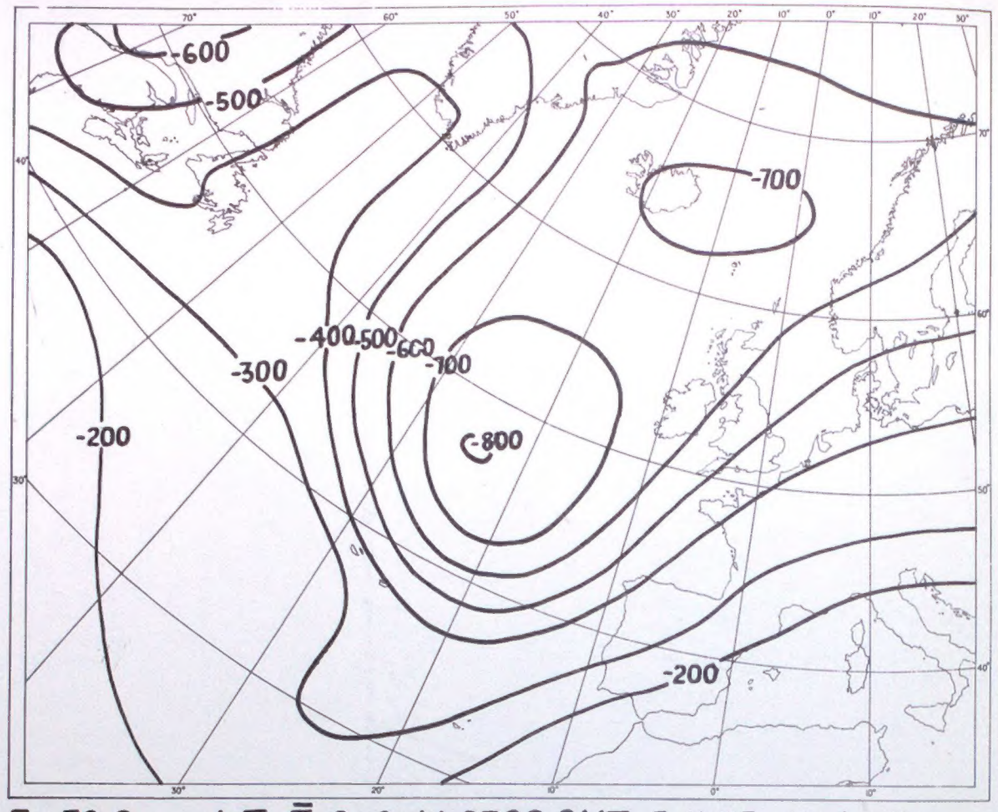

Fig.38. Original Z-$\bar{Z}$-G field 0300 G.M.T. 5:11:55 Units: ft.

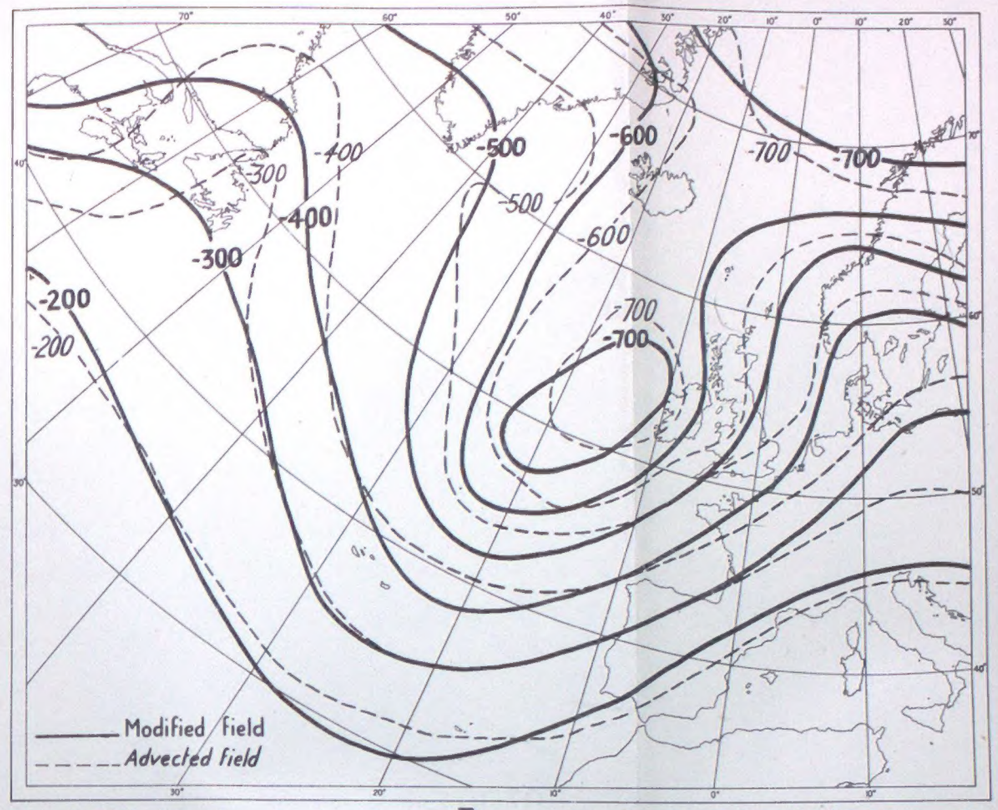

Fig.40. Modified and advected Z-$\bar{Z}$-G fields 0300 G.M.T. 5:11:55 Units: ft.

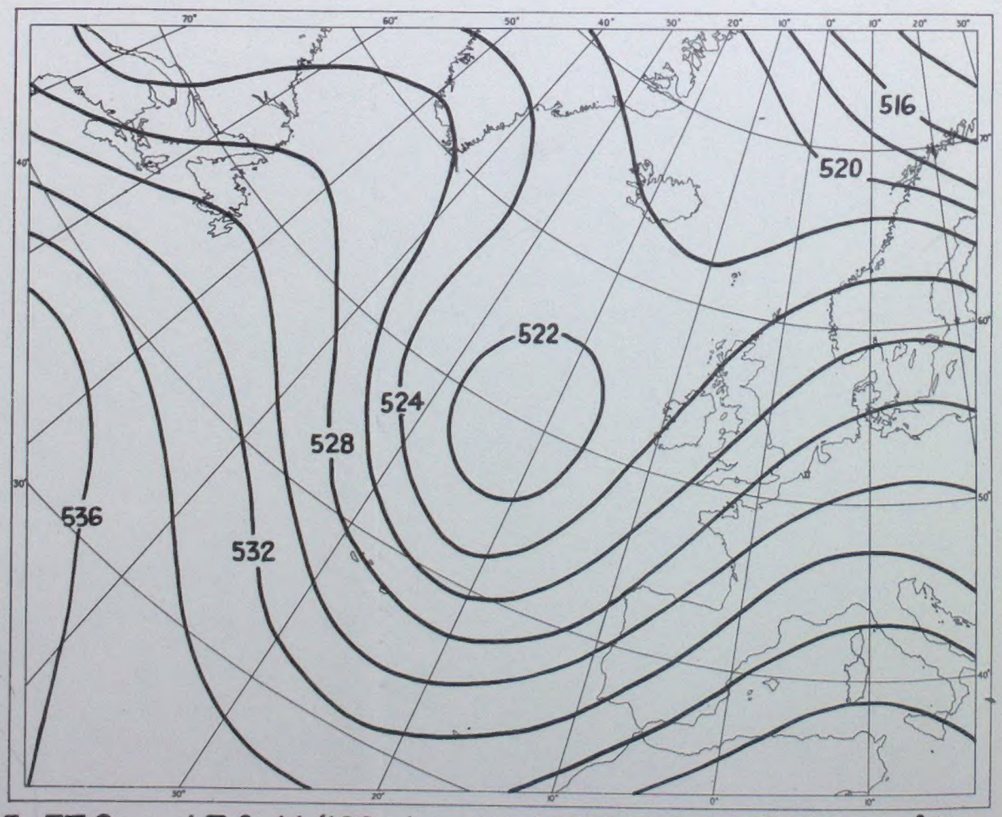

Fig.37. Original Z field (100 mb. contours) 0300 G.M.T. 5:11:55 Units: 10^2 Ft.

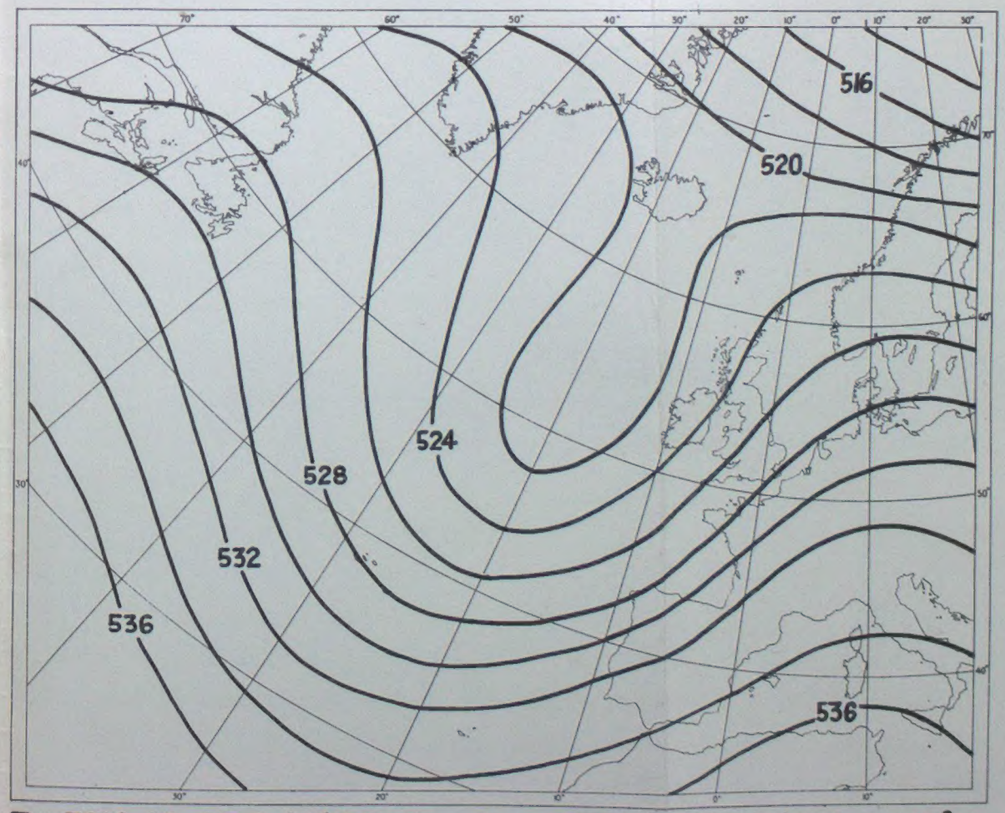

Fig.39. Modified Z field (100 mb. contours) 0300 G.M.T. 5:11:55 Units: 10^2 Ft

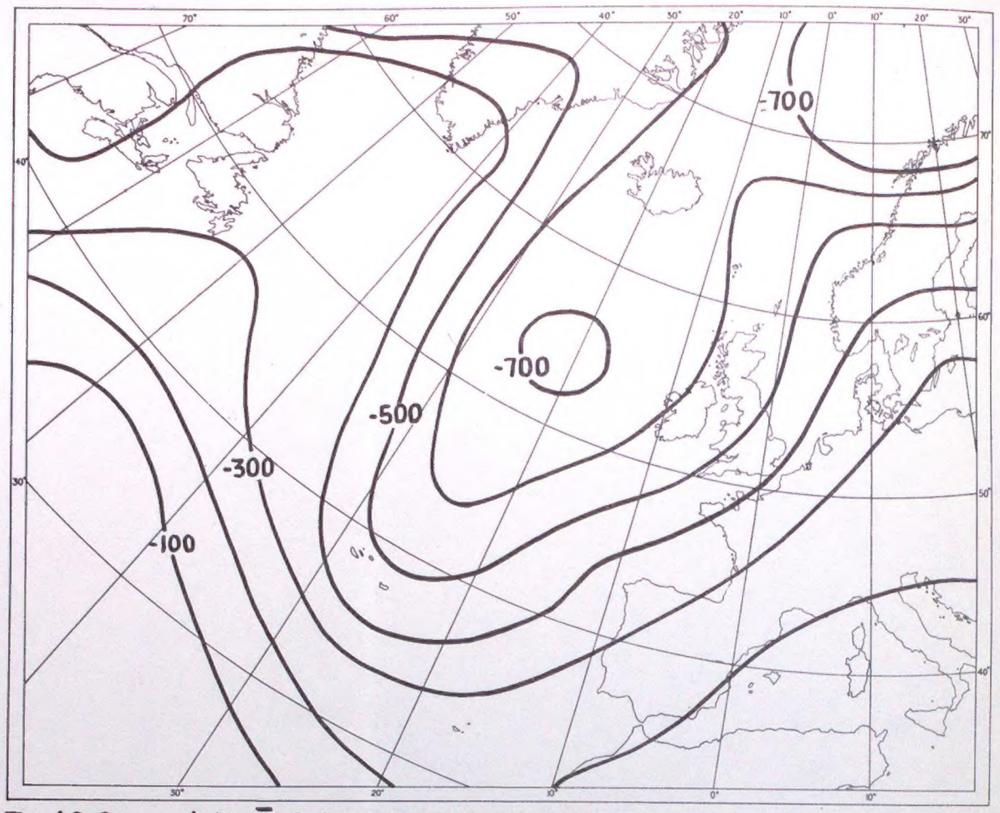

Fig.42. Original Z-$\bar{Z}$-G field 1500 G.M.T. 5:11:55 Units: Ft.

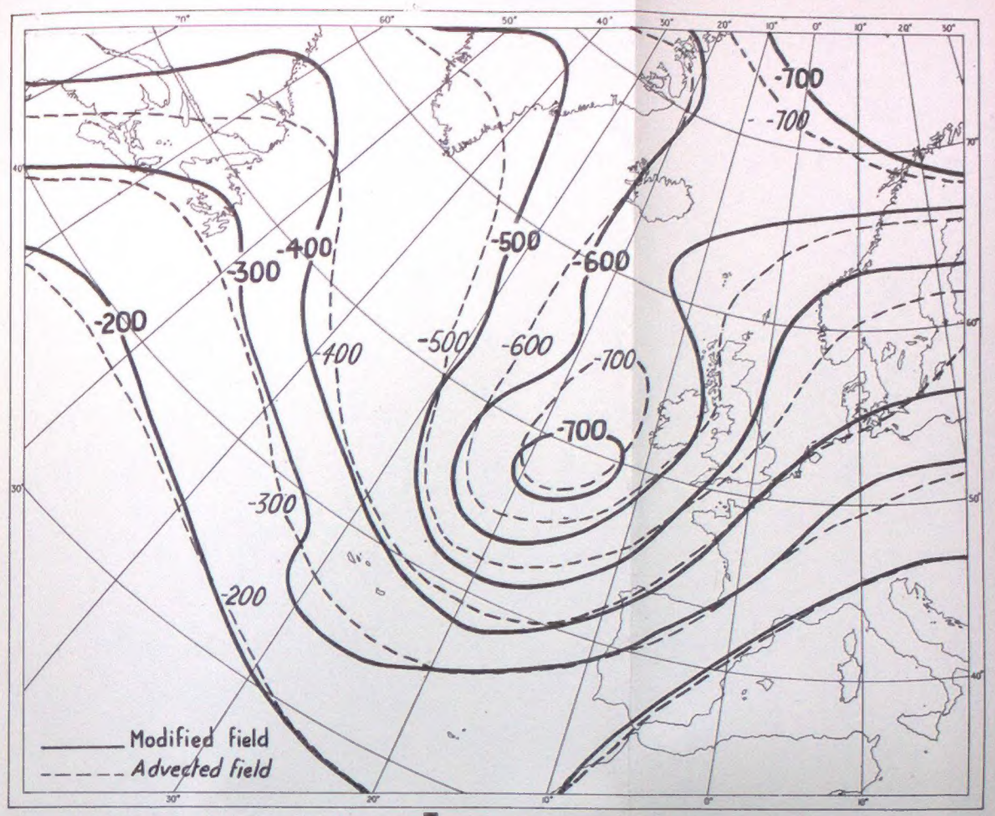

Fig.44. Modified and advected Z-$\bar{Z}$-G fields 1500 G.M.T. 5:11:55 Units: Ft.

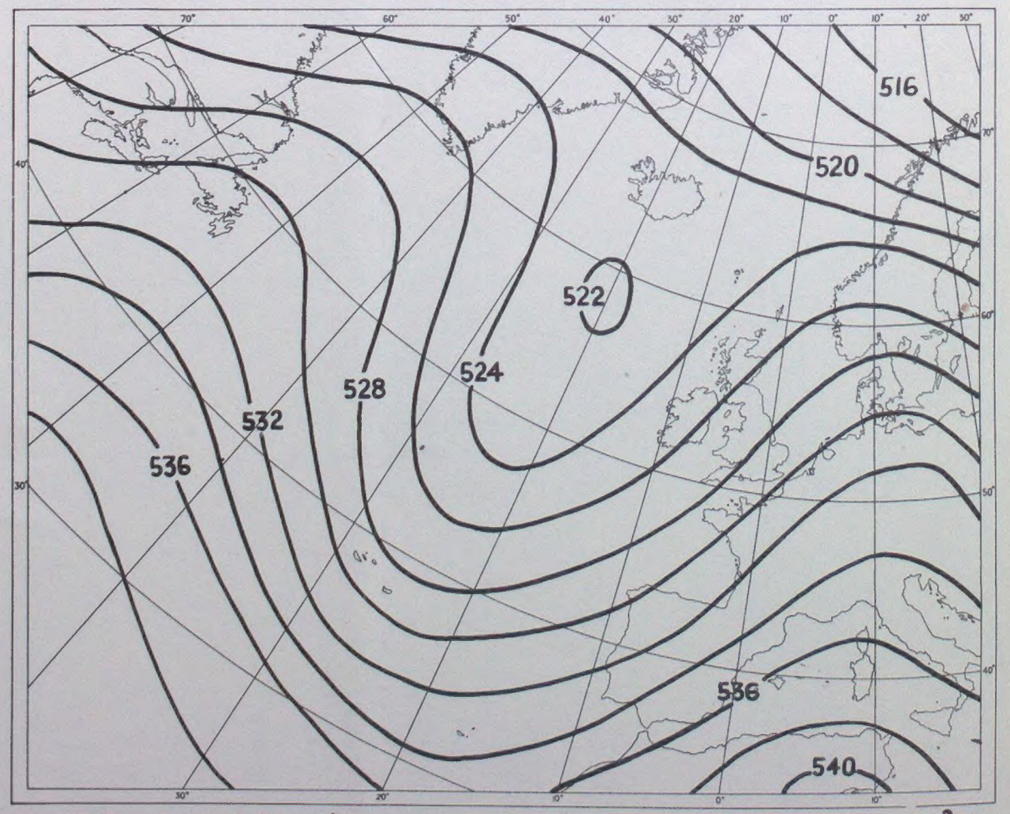

Fig.41. Original Z field (100mb. contours) 1500 G.M.T. 5:11:55 Units 10^2 Ft.

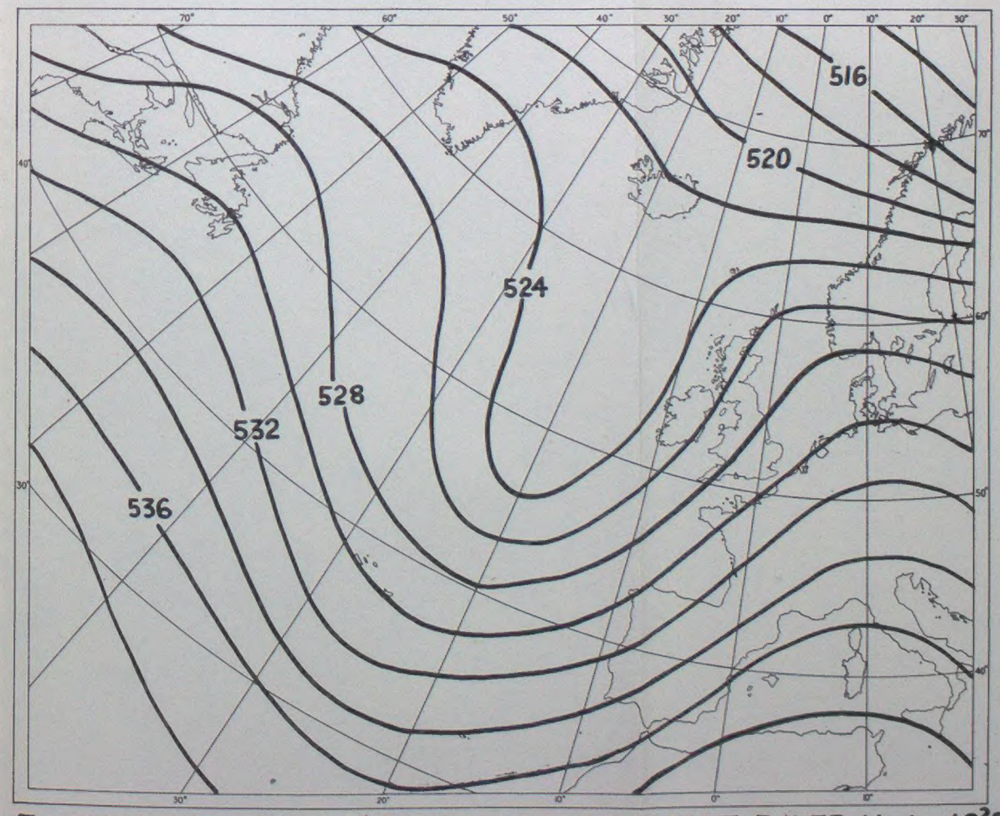

Fig.43. Modified Z field (100mb. contours) 1500 G.M.T. 5:11:55 Units: 10^2 Ft

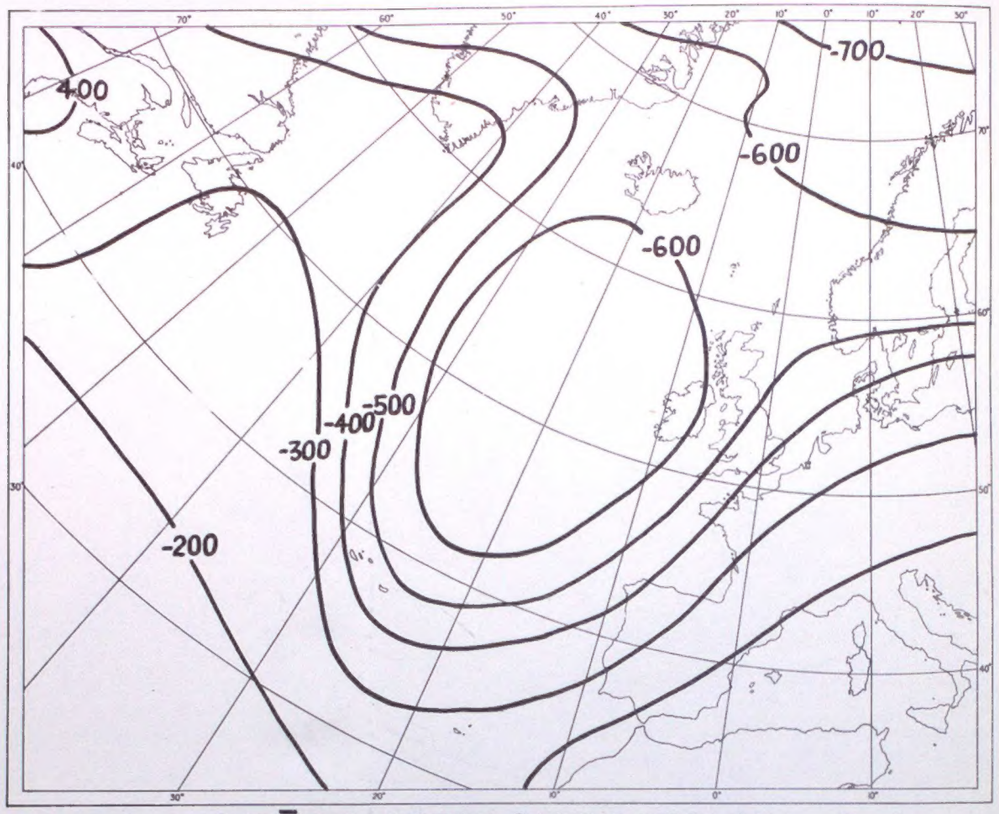

Fig.46. Original Z-$\bar{Z}$-G field 0300 G.M.T. 6:11:55 Units : ft.

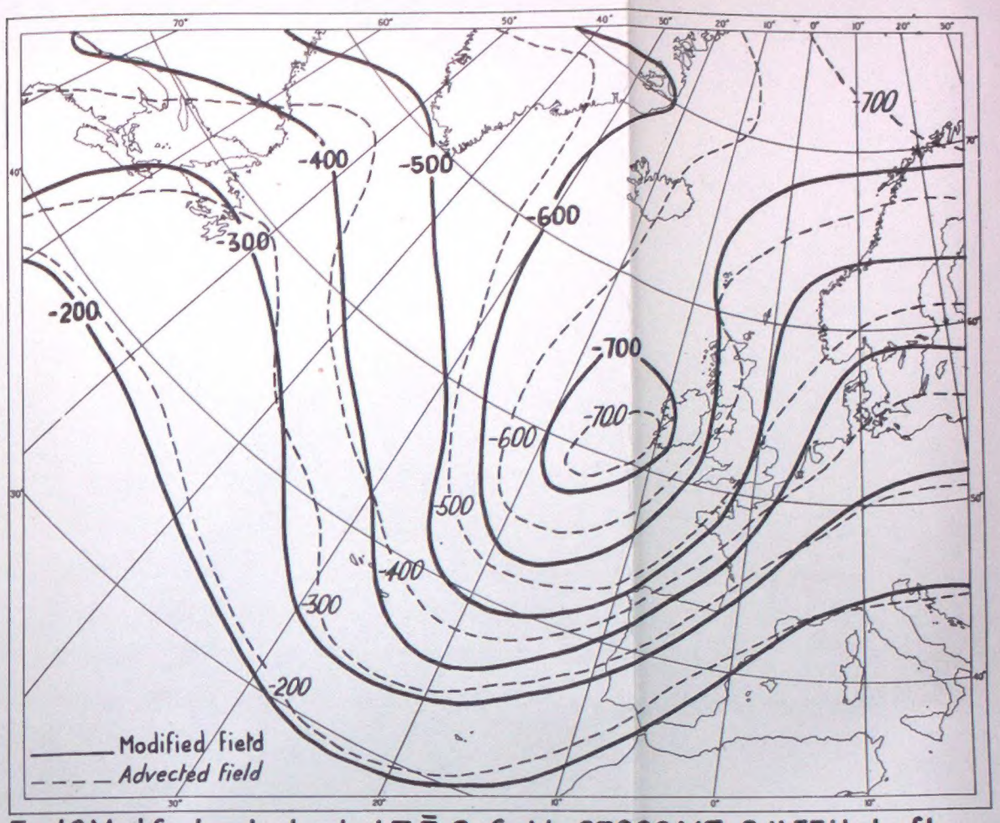

Fig.48 Modified and advected Z-$\bar{Z}$-G fields 0300 G.M.T. 6:11:55 Units: ft

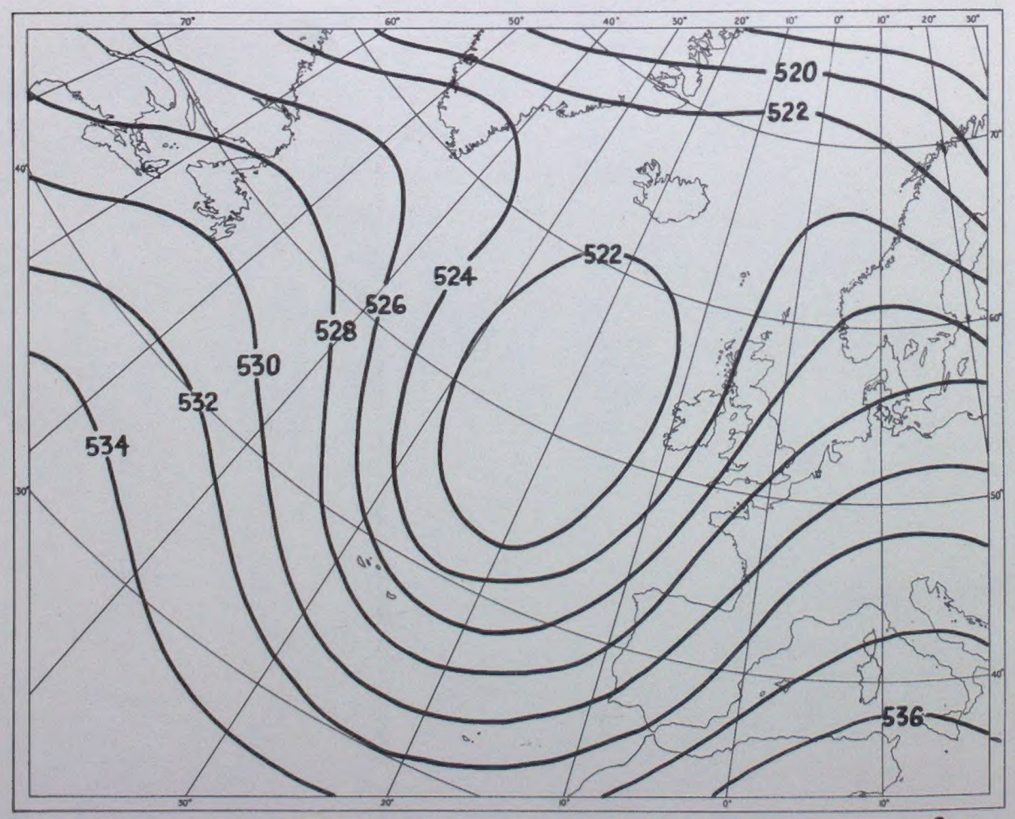

Fig.45. Original Z field (100mb. contours) 0300 G.M.T. 6:11:55 Units: 10^2 ft.

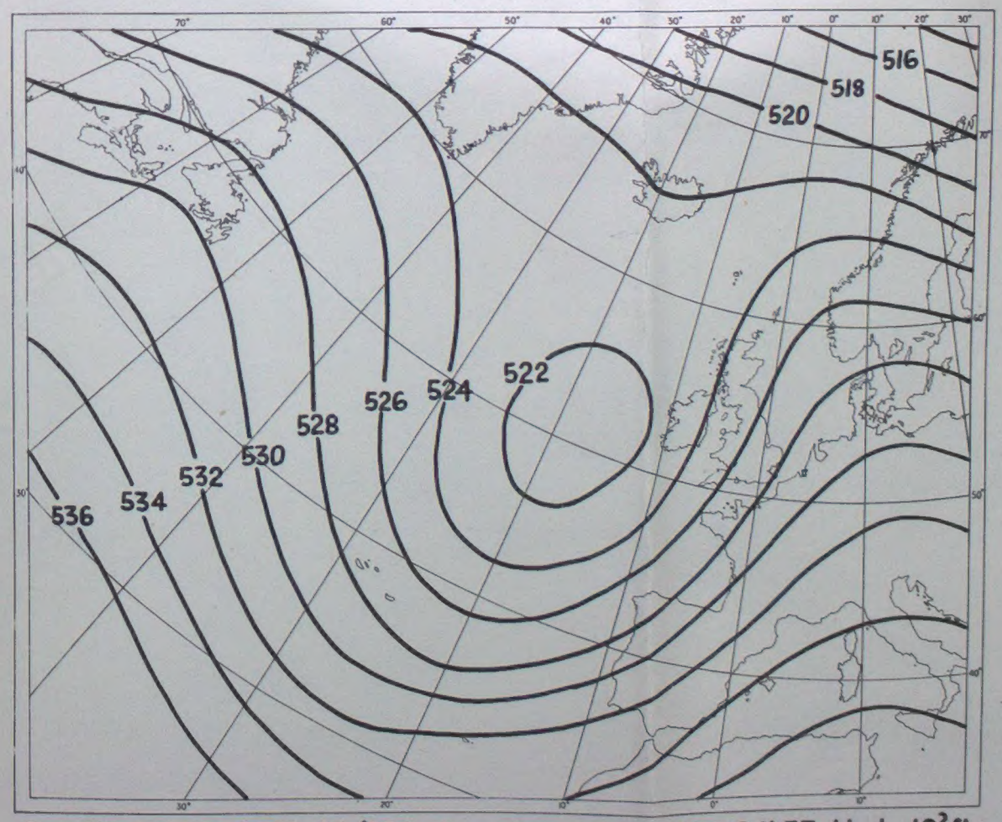

Fig. 47. Modified Z field (100mb. contours) 0300 G.M.T. 6:11:55 Units 10^2 ft.

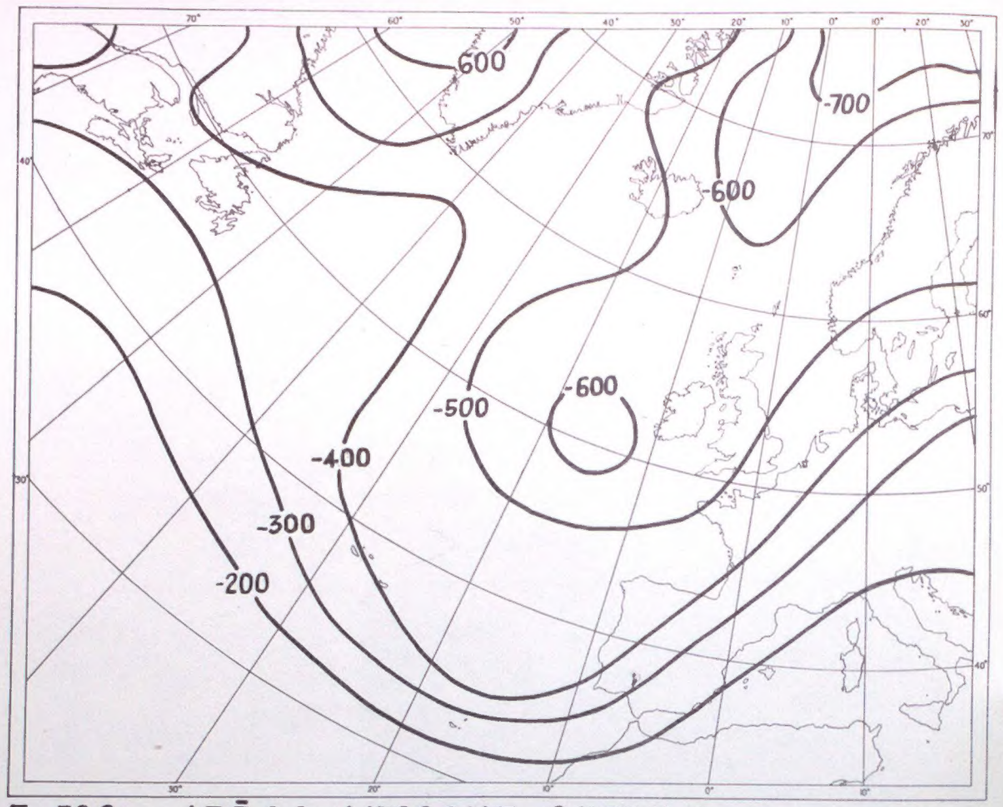

Fig.50 Original Z-$\bar{Z}$-G Field 1500 G.M.T. 6:11:55 Units : Ft.

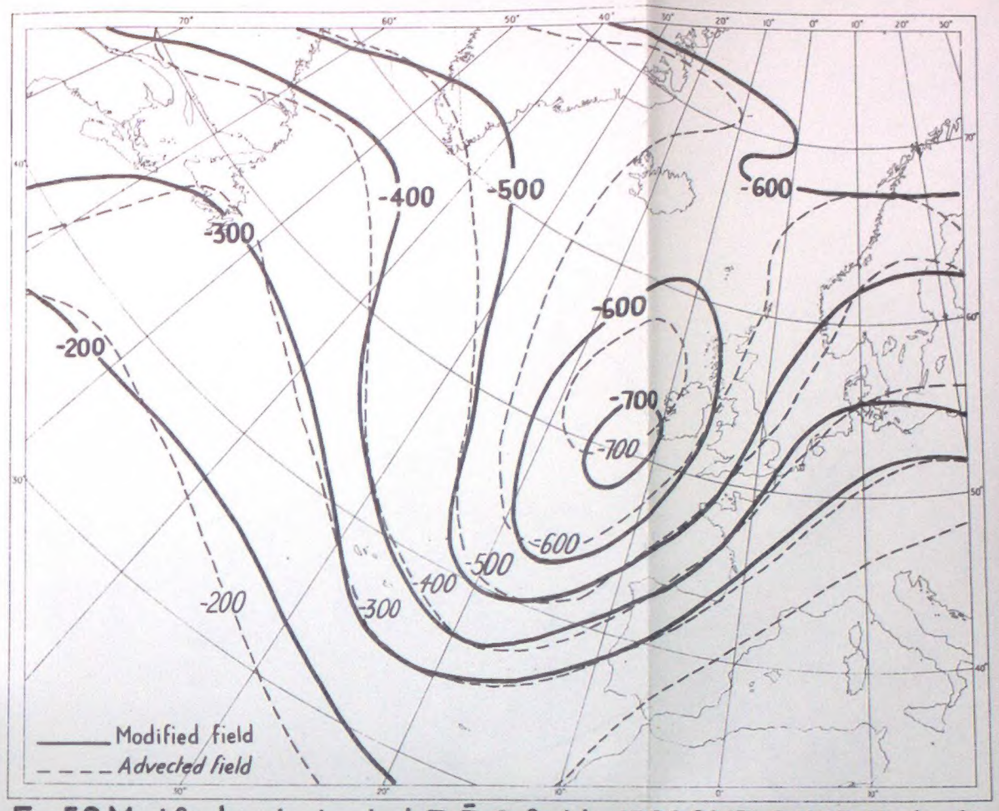

Fig.52 Modified and advected Z-$\bar{Z}$-G fields 1500 G.M.T. 6:11:55 Units : Ft.

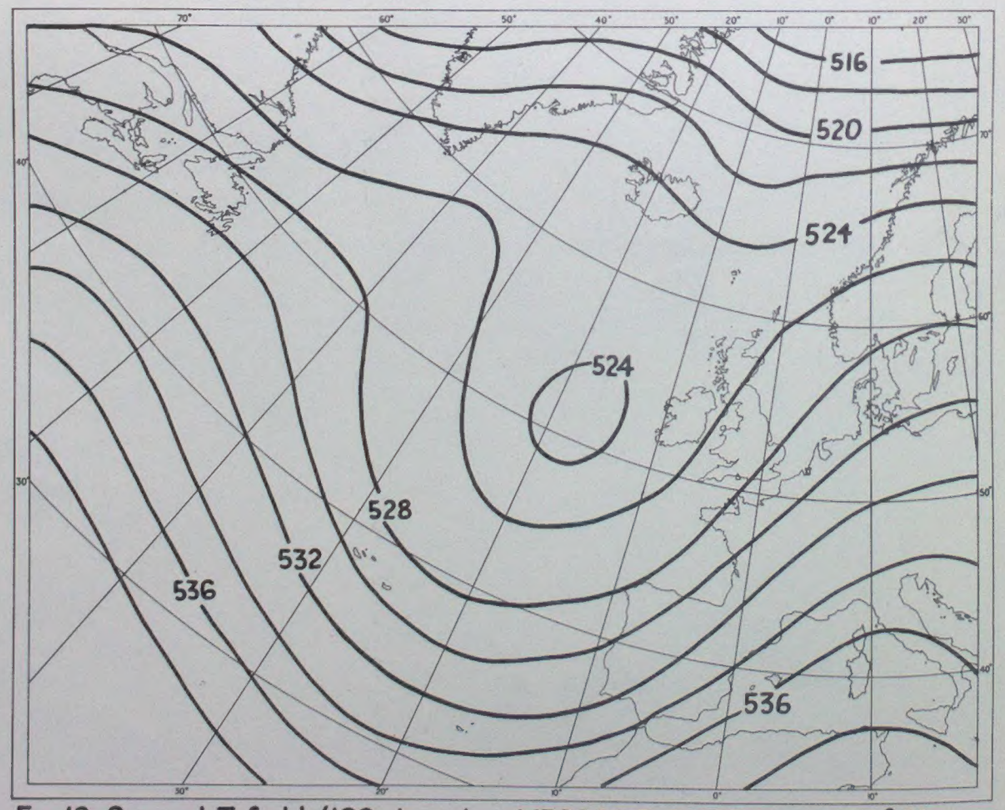

Fig.49. Original Z field (100mb. contours) 1500 G.M.T. 6:11:55 Units : 10^2 Ft.

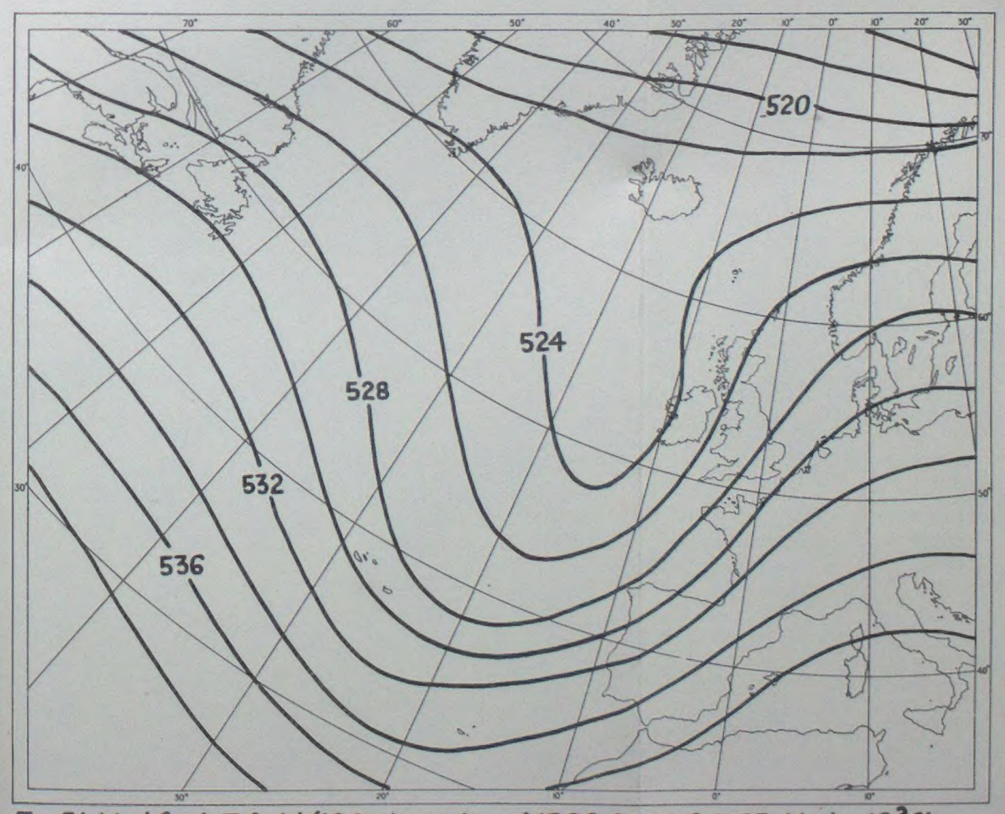

Fig.51. Modified Z field (100 mb. contours) 1500 G.M.T. 6:11:55 Units : 10^2 Ft.